

Parameterized TDOA: Instantaneous TDOA Estimation and Localization for Mobile Targets in a Time-Division Broadcast Positioning System

Chenxin Tu, Xiaowei Cui, Gang Lui, Sihao Zhao, *Senior Member, IEEE* and Mingquan Lu

Abstract—Localization of mobile targets is a fundamental problem across various domains. One-way ranging-based downlink localization has gained significant attention due to its ability to support an unlimited number of targets and enable autonomous navigation by performing localization at the target side. Time-difference-of-arrival (TDOA)-based methods are particularly advantageous as they obviate the need for target-anchor synchronization, unlike time-of-arrival (TOA)-based approaches. However, existing TDOA estimation methods inherently rely on the quasi-static assumption (QSA), which assumes that targets remain stationary during the measurement period, thereby limiting their applicability in dynamic environments. In this paper, we propose a novel instantaneous TDOA estimation method for dynamic environments, termed Parameterized TDOA (P-TDOA). We first characterize the nonlinear, time-varying TDOA measurements using polynomial models and construct a system of linear equations for the model parameters through dedicated transformations, employing a novel successive time difference strategy (STDS). Subsequently, we solve the parameters with a weighted least squares (WLS) solution thereby obtaining instantaneous TDOA estimates. Furthermore, we develop a mobile target localization approach that leverages instantaneous TDOA estimates from multiple anchor pairs at the same instant. Theoretical analysis shows that our proposed method can approach the Cramr-Rao lower bound (CRLB) of instantaneous TDOA estimation and localization in concurrent TOA scenarios, despite actual TOA measurements being obtained sequentially. Extensive numerical simulations validate our theoretical analysis and demonstrate the effectiveness of the proposed method, highlighting its superiority over state-of-the-art approaches across various scenarios.

Index Terms—TDOA, sequential measurements, localization, parameterized, mobile targets, CRLB.

I. INTRODUCTION

WIRELESS positioning systems have found extensive applications across various fields, including industrial automation [1], healthcare [2], transportation [3], and military combat [4]. These systems are indispensable in daily life, providing precise positioning information that enhances both

Chenxin Tu and Gang Lui are with the Department of Electronic Engineering, Tsinghua University, Beijing 100084, China (e-mail: tcx22@mails.tsinghua.edu.cn; lui_gang@tsinghua.edu.cn).

Xiaowei Cui and Mingquan Lu are with the Department of Electronic Engineering, Beijing National Research Center for Information Science and Technology, Tsinghua University, Beijing 100084, China (e-mail: cxw2005@tsinghua.edu.cn; lumq@tsinghua.edu.cn).

Sihao Zhao is with NovAtel, Autonomy & Positioning division of Hexagon, Calgary, AB T3K 2L5, Canada (e-mail: zsh01@tsinghua.org.cn).

Manuscript received XX XX, 2024. (*Corresponding author: Xiaowei Cui; Mingquan Lu*)

operational efficiency and safety. The most widely used wireless positioning systems are global navigation satellite systems (GNSSs), which, however, become ineffective in challenging environments such as urban canyons and indoor scenarios [5], [6]. In contrast, local positioning systems based on other wireless signals, such as ultra-wideband (UWB), are widely adopted in GNSS-denied environments [7]–[9].

A typical local positioning system consists of several anchors and multiple targets. Anchors are stationary reference points with known positions, while targets are stationary or mobile objects that need to be localized within the coordinate system established by the anchors. Localization measurements include time-of-arrival (TOA) [10]–[12], time-of-flight (TOF) [13], and time-difference-of-arrival (TDOA) [14]–[16], with various localization methods developed based on these measurements.

TOA-based methods require targets to synchronize with anchors, which is challenging to achieve. TOA-based methods also require synchronization or multiple instances of two-way ranging [17], adding significant communication overhead. Consequently, these methods are not suitable for large-scale networks and are impractical for passive targets. In contrast, time-difference-of-arrival (TDOA) methods for source localization do not require synchronization between targets and anchors. Anchors are pre-synchronized, and the differences in time-of-arrival (TOA) measurements across different anchors effectively eliminate the unknown transmission time of the targets. Such approaches have been extensively utilized in various applications.

Despite their advantages, source localization scheme faces two essential problems. On the one hand, source targets must occupy communication channels and transmit signals, which constrains the overall capacity of the positioning system. On the other hand, localization is typically performed on the central processing unit, rendering privacy problems. Therefore, numerous studies have focused on downlink TDOA estimation and localization in a time-division broadcast positioning system (TDBPS), where anchors broadcast signals in a time-division manner and targets passively receive them [14], [16]. Exemplified by ultrawide-band (UWB) device networks and acoustic sensor networks, Such systems have been widely employed in indoor and underwater scenarios. [8], [9], [18].

A. Challenges for TDOA Estimation

We observe two major challenges for TDOA estimation in a TDBPS. The first challenge lies in the asynchronous

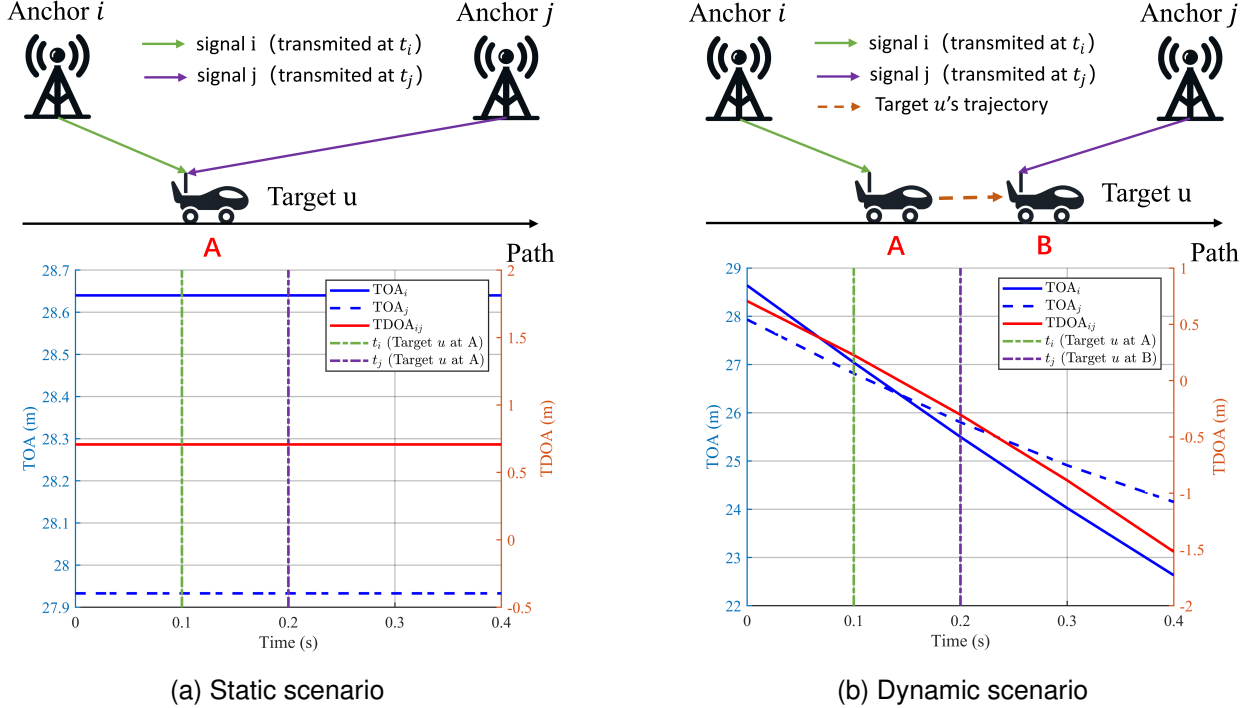


Fig. 1: TDOA measurement in two scenarios. (a) Static scenario: the target can be assumed to be stationary during the measurement period, allowing sequential TOA measurements at different times to correspond to the same position of Target u , which can be used for localization. (b) Dynamic scenario: the target cannot be assumed to be stationary, and displacement during the measurement period cannot be neglected. In this case, sequential TOA measurements at different times correspond to different positions of Target u , making localization impractical.

clocks between anchors and targets. Unlike source localization with concurrent TOA measurements, the clock offsets of a single target in different TOA measurements are not the same, as the TOA measurements are obtained sequentially at different times, preventing the elimination of clock offsets through differencing. Extensive research has been conducted to mitigate the impact of asynchronous clocks. Dotlic *et al.* utilize carrier frequency offset (CFO) measurements to reduce errors caused by asynchronous clocks in uplink TDOA [19], and [16] extends this approach to downlink TDOA scenarios. Zhang *et al.* [20], [21] employ the ratio of recorded intervals in local time over the same period to estimate the relative clock drift, thereby mitigating clock drift effects.

The second challenge lies in target mobility, which has received limited attention but is the focus of our research. We illustrate the downlink TDOA measurement process in a TDBPS in Fig. 1. Anchors i and j broadcast signals sequentially at t_i and t_j , respectively, with an interval of $T_s = t_j - t_i$, and the signals are subsequently received by Target u . We consider two scenarios. In Fig.1(a), Target u remains stationary at Point A, which we refer to as the static scenario. While in Fig. 1(b), Target u moves from Point A to Point B during the interval T_s . For simplicity, we neglect the influence of asynchronous clocks and timestamp noise. The range between Target u and Anchor $i(j)$ is represented by $TOA_{i(j)}$, depicted by blue curves, while the range difference is represented by $TDOA_{ij} = TOA_i - TOA_j$, depicted by

red curves. The sequential TOA measurements from different anchors are obtained at different times, with only $TOA_i(t_i)$ and $TOA_j(t_j)$ available.

In the cases where the anchors and target u are stationary, as shown in Fig. 1(a), TOA measurements are time-invariant, yielding

$$\begin{aligned} TDOA_{ij}(t_i) &= TOA_i(t_i) - TOA_j(t_i) = TDOA_{ij}(A) \\ TDOA_{ij}(t_j) &= TOA_i(t_j) - TOA_j(t_j) = TDOA_{ij}(A) \\ TDOA_{ij}(A) &= TOA_i(t_i) - TOA_j(t_j) \end{aligned} \quad (1)$$

In this way, the difference of sequential TOA measurements is the same as the difference of concurrent TOA measurements, corresponding to the TDOA between Target u and anchor pair (i, j) at a specific location. This relationship still holds approximately in scenarios where Target u is mobile but the displacement during the measurement period is negligible, such that it does not significantly affect TDOA estimation. We refer to such scenarios as quasi-static, which include cases where Target u moves slowly or the measurement period is extremely short. Existing TDOA estimation methods [16], [19]–[21] inherently rely on the fundamental assumption that targets remain stationary or exhibit quasi-static behavior during measurement periods, which we refer to as the quasi-static assumption (QSA). However, in many applications, the transmission intervals between different anchors are relatively long compared to the speed of the targets, making target mobility a non-negligible factor.

In contrast, when TOA measurements are time-variant, TOA measurements are time-variant, as shown in Fig. 1(b), we have

$$\begin{aligned} \text{TDOA}_{ij}(t_i) &= \text{TOA}_i(t_i) - \text{TOA}_j(t_i) = \text{TDOA}_{ij}(A) \\ \text{TDOA}_{ij}(t_j) &= \text{TOA}_i(t_j) - \text{TOA}_j(t_j) = \text{TDOA}_{ij}(B) \\ \text{TDOA}_{ij}(A) &\neq \text{TOA}_i(t_i) - \text{TOA}_j(t_j) \neq \text{TDOA}_{ij}(B) \end{aligned} \quad (2)$$

In dynamic scenarios, the difference between sequential TOA measurements does not correspond to the TDOA at any specific time or location, making it unsuitable for accurate localization.

To distinguish between these two scenarios, we define static scenarios as those where targets can be assumed to be stationary during the measurement period. Conversely, dynamic scenarios are characterized by significant target displacement during the measurement period, making the QSA inapplicable. Existing TDOA estimation methods based on QSA are unsuitable for dynamic scenes, and our work aims to address this gap.

B. Previous Work on Mobile Target localization

We have shown in Fig. 1(b) that the sequential TOA measurements correspond to pseudoranges from anchors to different positions of the mobile target, making them unsuitable for direct localization. There are two types of solutions to address this problem: one involves modeling the errors due to asynchronous clocks and target mobility, constructing equations with respect to the position at a specific instant; the other attempts to derive concurrent measurements from sequential ones.

For the first type of solutions, Shi *et al.* [22] propose an extended two-step WLS method to jointly estimate the position, velocity, clock drift, and clock offset of the mobile target. However, this method reparameterizes the localization problem into a higher-dimensional space, requiring additional anchors and increasing computational cost due to iterative optimization. Zhao *et al.* [23] develop a maximum likelihood (ML) based method that performs joint localization and synchronization through iterative processes. However, this iterative method requires a good initial guess and involves complex computations. Guo *et al.* [24] improve upon previous work by deriving a closed-form solution for joint localization and synchronization, eliminating the need for an initial guess and reducing the number of required anchors. However, the introduction of simultaneous quadratic equations may lead to cases where no real solutions exist, resulting in potential failures.

The aforementioned methods treat localization and synchronization as a coupled problem, jointly estimating clock parameters, position, and velocity. While constructing equations based on sequential TOA measurements is straightforward, solving these equations is challenging due to their nonlinearity. Moreover, joint estimation can degrade localization performance because of uncertainties introduced by additional parameters. Additionally, joint estimation increases the number of unknown variables, necessitating more anchors to obtain a unique solution. For instance, Shi's method requires at least nine anchors [22], whereas Guo's method requires at

least seven anchors, which is impractical in many real-world scenarios.

In contrast, the second type of solution circumvents these drawbacks. A timestamp conversion-based method is proposed in [25], employing Lagrange interpolation to convert sequential measurements to a unified reference instant, effectively transforming the problem into a GNSS-like scenario with concurrent TOA measurements. Although it has been proven that the timestamp conversion process does not introduce additional noise, the localization method used in the second step is suboptimal and fails to reach the Cramr-Rao lower bound (CRLB). Furthermore, Lagrange interpolation is equivalent to linear interpolation with only TOA measurements, which implicitly assumes constant velocity for the mobile target during the measurement period, potentially leading to performance degradation in highly dynamic scenarios.

C. Our Contributions

In dynamic scenarios, TDOA measurements are time-varying, making instantaneous TDOA estimation challenging, as it cannot be directly obtained from sequential TOA measurements. In addition, localization based on TDOA measurements has been well addressed in static scenarios. If we can obtain instantaneous TDOA measurements from several anchor pairs to the mobile target at the same instant, classical multilateration methods [26], [27], which have been shown to achieve the Cramr-Rao lower bound (CRLB) under small noise conditions, can be used to determine the instantaneous position of the mobile target. In summary, the core issue is to estimate instantaneous TDOAs from sequential TOA measurements, which has received little attention in prior research.

A similar challenge arises in instantaneous TOA estimation. Rajan *et al.* [28] develop a novel method for ranging in dynamic scenarios by modeling time-varying ranges as polynomial functions of time and converting the instantaneous TOA estimation problem into a parameter estimation problem for the polynomial coefficients. However, their method requires two-way ranging and is unsuitable for passive targets. A parameterized method for TDOA estimation under complex signal dynamics is introduced in [29], employing Taylor series and Fourier series to model nonlinear TDOA measurements. However, the nonlinearity in their research arises from signal propagation complexities through nonhomogeneous media, rather than target mobility.

In this paper, we first adopt the polynomial models of TOA measurements in [28], and further extend it by modeling the difference between two TOA measurements, i.e., TDOA measurements, as a polynomial function of time. Since the TOA model parameters cannot be directly solved in one-way communication scenarios, we apply specific transformations to combine the coefficients of the two TOA polynomial functions and identify the conditions under which this combination holds. This transforms the problem into estimating the parameters of the polynomial TDOA model. These identified conditions also provide guidelines for designing measurement protocols. Subsequently, we develop a method based on weighted least squares (WLS), called Mobile Weighted

Least Squares (MWLS), to estimate the TDOA parameters and thereby obtain instantaneous TDOA estimates. We observe that constructing equations using traditional approaches by taking TOA differences within the same frame leads to an ill-posed WLS problem. To resolve this, we propose a novel strategy called the Successive Time Difference Strategy (STDS) for constructing equations, ultimately rendering the problem solvable.

Our contributions and innovations are summarized as follows:

- We propose a novel method for instantaneous TDOA estimation in dynamic scenarios called Parameterized TDOA (P-TDOA). This method utilizes a polynomial model to approximate the nonlinear, time-varying TDOA measurements. To obtain instantaneous TDOA estimates, we introduce a novel time difference strategy and a WLS solution.
- We present an effective mobile target localization method based on multiple instantaneous TDOA estimates using P-TDOA. By decoupling localization from synchronization, this method achieves higher positioning accuracy while requiring fewer anchors. Additionally, by selecting a higher model order, our method can be adapted to highly dynamic scenarios.

Theoretical analysis and extensive numerical simulations demonstrate the effectiveness of our proposed methods. Unlike existing approaches, P-TDOA can be applied in both dynamic and static scenarios. Although TOA measurements are obtained sequentially, the performance of P-TDOA can approach the Cramér-Rao lower bound (CRLB) of TDOA estimation and localization under concurrent TOA scenarios. The proposed mobile target localization method exhibits higher accuracy, reduced anchor requirements, and greater robustness to variations in anchor and target distributions compared to state-of-the-art methods.

The rest of the paper is organized as follows. In Section II, we formulate our problem, including the measurement models for asynchronous clocks and timestamps, as well as the time-division (TD) protocol adopted. The proposed P-TDOA is detailed in Section III, including the polynomial TDOA model and methods for TDOA estimation and mobile target localization. In Section IV, we derive the CRLB of instantaneous TDOA estimation and localization, as well as the theoretical mean square error (MSE) of P-TDOA. Extensive simulations to evaluate the effectiveness of our proposed method are presented in Section V. Finally, our conclusions are summarized in Section VI.

The main notations and abbreviations used throughout this paper are summarized in Table I and Table II, respectively.

II. PROBLEM FORMULATION

We consider a TDBPS in K -dimensional ($K = 2$ or 3) scenario, consisting of N_a stationary anchors indexed from 1 to N_a ($\mathcal{N}_a = \{1, 2, \dots, N_a\}$) and multiple mobile targets. To simplify the illustration, we focus on a single mobile target, indexed by u , without loss of generality. As depicted in Fig. 2, the stationary anchors sequentially broadcast signals,

TABLE I: Notation List

Notation	Description
lowercase x	scalar
bold lowercase \mathbf{x}	vector
bold uppercase \mathbf{X}	matrix
i, j	indices of anchors
k	index of the target
c	the speed of light
N_a	number of anchors
N_p	number of anchor pairs
\mathcal{N}_a	set of anchors' indices, $\mathcal{N}_a = \{1, 2, \dots, N_a\}$
\mathcal{N}_p	set of anchors pairs' indices
$[\mathcal{N}]_i$	the i -th element of set \mathcal{N}
$[\mathbf{X}]_{i,j}$	entry at the i -th row and the j -th column of a matrix
$\mathbb{E}[\cdot]$	expectation operator
\mathbb{R}	set of real numbers
\mathbb{N}^+	set of positive integers
$\text{diag}(\cdot)$	diagonal matrix with the entries inside
\mathbf{V}^\dagger	left inverse of matrix \mathbf{V}
$(\cdot)^T$	transpose operator
$(\cdot)^{\odot N}$	element-wise matrix exponent
$\mathbf{0}_M$	vector with all entries being zero
$\mathbf{1}_M$	$M \times 1$ vector with all entries being one
$\mathbf{O}_{M \times N}$	$M \times N$ matrix with all entries being zero
\mathbf{I}_M	$M \times M$ identity matrix

TABLE II: Abbreviation List

Abbreviation	Full Name
CRLB	Cramér-Rao Lower Bound
LS	Least Squares
MSE	Mean Square Error
MWLS	Mobile Weighted Least Squares
P-TDOA	Parameterized Time-Difference-of-Arrival
RMSE	Root Mean Square Error
STDS	Successive Time Difference Strategy
TD	Time-Division
TDBPS	Time-Division Broadcast Positioning System
TDOA	Time-Difference-of-Arrival
TOA	Time-of-Arrival
WLS	Weighted Least Squares

which are then passively received by Target u . All anchors and targets are equipped with independent oscillators and wireless communication devices. The clocks of the anchors are assumed to be synchronized through wired or wireless means with minor synchronization errors, and their positions are known with some uncertainty. In contrast, the clocks of mobile targets are unsynchronized, and their positions are time-varying and unknown.

In the remainder of this section, we introduce the measurement models employed in this study, including the affine clock model and the timestamp measurement model. Subsequently, we present the TD protocol adopted by the system and describe the messages broadcast by the anchors.

A. Measurement Model

To address the issue of synchronization between anchors and targets, we first formulate the error model of asynchronous clocks. Anchors and targets, collectively referred to as nodes, are typically equipped with independent clock oscillators. Ideally, all clocks should be synchronized with a global reference time. However, due to oscillator imperfections and environmental conditions, non-linear deviations from ideal clocks occur. Although these deviations are inherently nonlinear, for

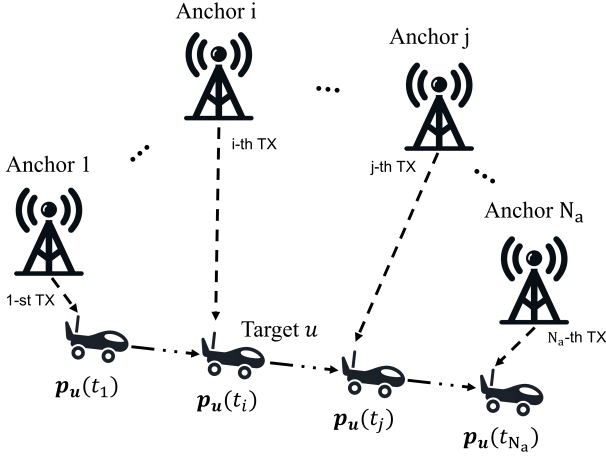


Fig. 2: Sequential signal transmission and reception in a TDBPS, where anchors broadcast signals sequentially, and the target passively receives them. The position and clock offset of the moving target change over time.

typical oscillators with small Allan deviations, common in practice, they can be effectively modeled as linear errors over short periods [30]. Thus, the relationship between Node i 's local time t_i and global time t can be modeled as

$$\begin{aligned} t_i &= t + \phi_i(t) \\ &= (1 + e_i)t + \phi_i = \omega_i t + \phi_i \end{aligned} \quad (3)$$

where $\phi_i(t)$ represents the clock offset of Node i at t , while e_i , ω_i and ϕ_i denote the relative clock frequency deviation, the clock drift and the initial clock offset of Node i , respectively. We convert the global time t to the local time t_i by

$$t = \mathcal{G}(t_i) = \alpha_i t_i + \beta_i \quad (4)$$

where $[\alpha_i, \beta_i] \triangleq [\omega_i^{-1}, -\phi_i \omega_i^{-1}]$ are the calibration parameters. For ideal clocks that are well synchronized with the global time, we have $[\omega_i, \phi_i] = [1, 0]$ and $[\alpha_i, \beta_i] = [1, 0]$.

Anchors and targets can record transmission and reception time in their local time coordinates. Generally, the noise in transmission and reception timestamps typically differs in magnitude; thus, we denote them by v and w , respectively. The timestamp measurements are modeled as follows

$$\begin{aligned} \hat{t}_i^{TX} &= t_i^{TX} + v_i \\ \hat{t}_{ui}^{RX} &= t_{ui}^{RX} + w_{ui} \end{aligned} \quad (5)$$

where the superscripts TX and RX denote transmission and reception, respectively, and the subscript i indicates that the transmission timestamp and corresponding noise belong to Node i , while the subscript ui indicates that the reception timestamp is recorded by Node u for the signal transmitted by Node i . Typically, The timestamp measurement noise is assumed to follow a Gaussian distribution [20], [21].

B. TD Protocol

We assume that the anchors in the system operate in a periodic TD manner, where anchors broadcast signals at predetermined intervals, and the targets passively receive them.

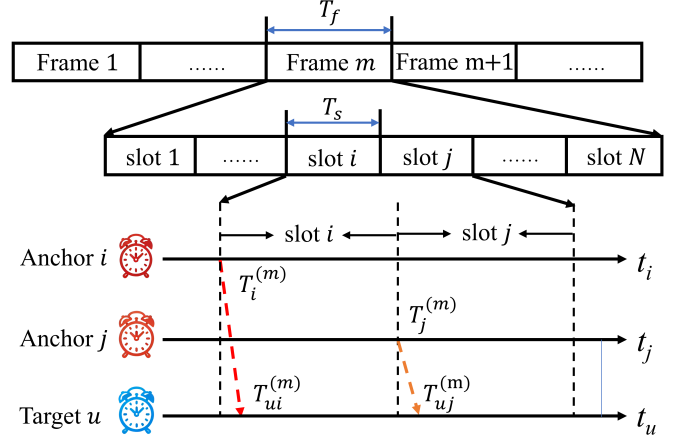


Fig. 3: Periodic broadcast TD protocol

The schematic diagram of the protocol is shown in Fig. 3¹. The minimal operational period, referred to as a frame, has a duration denoted as T_f . Each frame is subdivided into N time slots ($N \geq N_a$), with each slot having a duration of T_s . Each anchor occupies a unique slot and broadcasts signals at the beginning of its designated slot. The adopted protocol is similar to those described in [20], [21] and D-TDMA scheduling in [31].

Our problem requires only the transmission timestamps from the anchors and the reception timestamps from the targets. For simplicity, unless otherwise specified, the timestamps from an anchor refer to its transmission timestamps, and the timestamps from a target refer to its reception timestamps, allowing us to omit the superscripts TX and RX . Consider the signal transmitted by Anchor i in the m -th frame. The transmission timestamp recorded by Anchor i is denoted as $\hat{T}_i^{(m)}$, where $\hat{T}_i^{(m)} = T_i^{(m)} + v_i^{(m)}$, and $T_i^{(m)}$ and $v_i^{(m)}$ represent the actual local transmission time and measurement noise, respectively. Similarly, the reception timestamp recorded by Target u is denoted as $\hat{T}_{ui}^{(m)}$, where $\hat{T}_{ui}^{(m)} = T_{ui}^{(m)} + w_{ui}^{(m)}$, and $T_{ui}^{(m)}$ and $w_{ui}^{(m)}$ represent the actual local reception time and measurement noise, respectively.

Furthermore, signals broadcast by the anchors carry messages containing transmission timestamps, estimated clock offsets with uncertainties, and estimated positions with uncertainties². Taking Anchor i and Target u in Fig. 3 as an example, Anchor i occupies slot i in Frame m . At the start of slot i , Anchor i broadcasts a message containing:

- The transmission timestamp $T_i^{(m)}$.
- The estimated clock offset at the start of slot i $\hat{\phi}_i^{(m)}$ with its standard deviation $\sigma_{\phi_i^{(m)}}$.
- The estimated position $\hat{\mathbf{p}}_i$ with covariance matrix $\Sigma_{\mathbf{p}_i}$.

¹It is worth mentioning that our proposed P-TDOA method is not limited to the periodic broadcast protocol but can function under other TD protocols as well. We adopt this protocol for its widespread application and ease of illustration.

²The estimated clock offsets and positions are assumed to be contaminated by Gaussian noise, characterized by their standard deviations. This information is predetermined by the anchors.

These messages are essential for TDOA estimation and localization, which will be discussed in subsequent sections.

There are two main problems to address in the system. First, we aim to accurately estimate the instantaneous TDOAs between pairs of anchors and the mobile target within the communication range in dynamic scenarios, utilizing the affine clock model introduced in (3) and (4), along with the timestamp measurement model in (5). Next, we seek to localize the mobile target based on the estimated TDOAs. The methods for addressing these problems are presented in Section III-B and Section III-C, respectively.

III. PARAMETERIZED TDOA

In this section, we present our method for instantaneous TDOA estimation and localization of mobile targets. First, we derive a polynomial TDOA model inspired by the study from [28] in Section III-A. Next, we introduce a novel method for instantaneous TDOA estimation in Section III-B. Finally, based on the instantaneous TDOA estimates obtained, we develop a localization method for mobile targets in Section III-C.

A. Parameterized TDOA Model

To address the challenge of estimating time-varying TOAs, Rajan *et al.* approximate the non-linear time-varying ranges using polynomial functions derived from the Taylor series over short periods [28]. Under the true time coordinate, the TOA between Node i and Node j at global time t can be expressed as

$$\begin{aligned}\tau_{ij}(t) &\triangleq c^{-1}\mathcal{R}_{ij}(t) \\ &= c^{-1}\left(r_{ij}^{(0)} + \dots + r_{ij}^{(L-1)}t^{L-1} + O(t^L)\right)\end{aligned}\quad (6)$$

where $\mathcal{R}_{ij}(t)$ represents the time-varying range between Node i and Node j , $\mathbf{r}_{ij} = [r_{ij}^{(0)}, \dots, r_{ij}^{(L-1)}]^T \in \mathbb{R}^{L \times 1}$ denotes the range coefficients of the Taylor series expansion. Here, L denotes the number of parameters, corresponding to the model order plus one. The term $O(t^L)$ denotes the high-order error.

Although the relationships between transmission times, reception times, and TOAs are defined under the global time coordinate, the actual measured timestamps are recorded in local time using each node's independent clock oscillators. By substituting (4) into (6), we convert the TOA expression into Node j 's local time t_j , resulting in:

$$\begin{aligned}\tau_{ij}(t_j) &\triangleq c^{-1}\mathcal{R}_{ij}(\mathcal{G}(t_j)) \\ &= c^{-1}\left(r_{ij}^{(0)} + \dots + r_{ij}^{(L-1)}\mathcal{G}(t_j)^{L-1} + O(t_j^L)\right) \\ &= \left(\gamma_{ij}^{(0)} + \dots + \gamma_{ij}^{(L-1)}t_j^{L-1} + O(t_j^L)\right) \\ &= \boldsymbol{\nu}_{t_j}^T \boldsymbol{\gamma}_{ij} + O(t_j^L)\end{aligned}\quad (7)$$

where $\boldsymbol{\gamma}_{ij} = [\gamma_{ij}^{(0)}, \dots, \gamma_{ij}^{(L-1)}]^T \in \mathbb{R}^{L \times 1}$ denotes the coefficients of the TOA between Node i and Node j and $\boldsymbol{\nu}_{t_j} = [t_j^0, \dots, t_j^{L-1}]^T$ is the vector of powers of t_j from order zero to order $L-1$.

We then extend the parameterized model to TDOAs. Polynomial models are employed to characterize the time-varying

TDOAs in dynamic scenarios, which are inherently nonlinear but can be effectively approximated over short periods. We denote the TDOA between Target u and anchor pair (i, j) as $\tau_{u;ij}$. The parameterized model for the TDOA $\tau_{u;ij}$ at Node u 's local time t_u is formulated as

$$\begin{aligned}\tau_{u;ij}(t_u) &= \tau_{ui}(t_u) - \tau_{uj}(t_u) \\ &= \boldsymbol{\nu}_{t_u}^T (\boldsymbol{\gamma}_{ui} - \boldsymbol{\gamma}_{uj}) + O(t_u^L) \\ &= \boldsymbol{\nu}_{t_u}^T \boldsymbol{\gamma}_{u;ij} + O(t_u^L)\end{aligned}\quad (8)$$

where $\boldsymbol{\gamma}_{u;ij} = \boldsymbol{\gamma}_{ui} - \boldsymbol{\gamma}_{uj} = [\gamma_{u;ij}^{(0)}, \dots, \gamma_{u;ij}^{(L-1)}]^T$ denotes the coefficients of the TDOA $\tau_{u;ij}$.

B. Instantaneous TDOA Estimation

Although the polynomial TDOA model given by (8) is an extension of the TOA model in (6) and (7), the parameter estimation process is significantly more challenging, because we can only obtain sequential TOA measurements, i.e., τ_{ui} and τ_{uj} in (8), at different times. In this subsection, we first apply dedicated transformations to combine the coefficients of the two TOA polynomial functions, converting the problem into one of estimating the parameters of the TDOA model. We then solve these parameters using MWLS. However, constructing equations using traditional differences between TOAs within the same frame as in [16], [21], makes the WLS problem ill-posed. To address this issue, we propose an innovative and counterintuitive strategy called STDS, which ensures that the problem yields unique solutions.

1) *Mobile Weighted Least Square*: Consider a pair of stationary anchors (i, j) , where $i < j$, and a mobile target u . We take the m -th message transmitted by Anchor i and received by Target u as an example. Under ideal circumstances, assuming that all nodes are well synchronized and the recorded timestamps are noise-free, the timestamps are related by

$$T_i^{(m)} + \tau_{ui}(T_i^{(m)}) = T_{ui}^{(m)} \quad (9)$$

where $\tau_{ui}(T_i^{(m)})$ is defined in (6) and represents the TOA between Anchor i and Target u at $T_i^{(m)}$. We make a fundamental assumption that due to the short TOA duration³, the displacement of Target u during the air time can be ignored, i.e., $\tau_{ui}(T_i^{(m)}) = \tau_{ui}(T_{ui}^{(m)})$. For simplicity, we abbreviate $\tau_{ui}(T_i^{(m)})$ as $\tau_{ui}^{(m)}$. When considering non-ideal clocks, substituting (3) into $T_i^{(m)}$ and (4) into $T_{ui}^{(m)}$ in (9), respectively, yields the following result.

$$T_i^{(m)} - \phi_i^{(m)} + \tau_{ui}^{(m)} = \alpha_u T_{ui}^{(m)} + \beta_u \quad (10)$$

Similarly, we can derive another equation for the n -th message transmitted by Anchor j and received by Target u , given by

$$T_j^{(n)} - \phi_j^{(n)} + \tau_{uj}^{(n)} = \alpha_u T_{uj}^{(n)} + \beta_u \quad (11)$$

We observe that the TOA measurements are coupled with the unknown clock parameters of Target u . To eliminate the unknown parameter β_u , subtracting (10) from (11) yields

$$(T_i^{(m)} - \phi_i^{(m)}) - (T_j^{(n)} - \phi_j^{(n)}) + (\tau_{ui}^{(m)} - \tau_{uj}^{(n)}) = \alpha_u (T_{ui}^{(m)} - T_{uj}^{(n)}) \quad (12)$$

³The range of 300m corresponds to an approximate time delay of 1 μ s, which is significantly shorter than the transmission intervals.

$$[(T_i^{(m)} - \phi_i^{(m)}) - (T_j^{(n)} - \phi_j^{(n)})](T_{ui}^{(p)} - T_{uj}^{(q)}) - [(T_i^{(p)} - \phi_i^{(p)}) - (T_j^{(q)} - \phi_j^{(q)})](T_{ui}^{(m)} - T_{uj}^{(n)}) + [(\tau_{ui}^{(m)} - \tau_{uj}^{(n)})](T_{ui}^{(p)} - T_{uj}^{(q)}) - (\tau_{ui}^{(p)} - \tau_{uj}^{(q)})(T_{ui}^{(m)} - T_{uj}^{(n)})] = 0 \quad (15)$$

$$\begin{aligned} & [(T_i^{(m)} - \phi_i^{(m)}) - (T_j^{(n)} - \phi_j^{(n)})](T_{ui}^{(p)} - T_{uj}^{(q)}) - [(T_i^{(p)} - \phi_i^{(p)}) - (T_j^{(q)} - \phi_j^{(q)})](T_{ui}^{(m)} - T_{uj}^{(n)}) + \\ & \sum_{l=0}^{L-1} \gamma_{ui}^{(l)} \underbrace{[T_{ui}^{(m)}]^l (T_{ui}^{(p)} - T_{uj}^{(q)}) - T_{ui}^{(p)l} (T_{ui}^{(m)} - T_{uj}^{(n)})}_{a_{l,ui}^{(m,n,p,q)}} - \gamma_{uj}^{(l)} \underbrace{[T_{uj}^{(n)}]^l (T_{ui}^{(p)} - T_{uj}^{(q)}) - T_{uj}^{(q)l} (T_{ui}^{(m)} - T_{uj}^{(n)})}_{a_{l,uj}^{(m,n,p,q)}} + \\ & \underbrace{\left[O(T_{ui}^{(m)l}) (T_{ui}^{(p)} - T_{uj}^{(q)}) - O(T_{ui}^{(p)l}) (T_{ui}^{(m)} - T_{uj}^{(n)}) + O(T_{uj}^{(q)l}) (T_{ui}^{(m)} - T_{uj}^{(n)}) - O(T_{uj}^{(n)l}) (T_{ui}^{(p)} - T_{uj}^{(q)}) \right]}_{O_t} = 0 \end{aligned} \quad (16)$$

In (12), the unknown α_u still exists. To eliminate α_u , following the pattern of (12), we can write another equation for the p -th message from Anchor i and the q -th message from Anchor j as:

$$(T_i^{(p)} - \phi_i^{(p)}) - (T_j^{(q)} - \phi_j^{(q)}) + (\tau_{ui}^{(p)} - \tau_{uj}^{(q)}) = \alpha_u (T_{ui}^{(p)} - T_{uj}^{(q)}) \quad (13)$$

By dividing equation (12) by equation (13), we can eliminate α_u and obtain a simplified relationship.

$$\frac{(T_i^{(m)} - \phi_i^{(m)}) - (T_j^{(n)} - \phi_j^{(n)}) + (\tau_{ui}^{(m)} - \tau_{uj}^{(n)})}{(T_i^{(p)} - \phi_i^{(p)}) - (T_j^{(q)} - \phi_j^{(q)}) + (\tau_{ui}^{(p)} - \tau_{uj}^{(q)})} = \frac{T_{ui}^{(m)} - T_{uj}^{(n)}}{T_{ui}^{(p)} - T_{uj}^{(q)}} \quad (14)$$

Finally, we have eliminated the unknown clock parameters of Target u . By rearranging equation (14), we obtain (15). Next, substituting the polynomial TOA model in (7) into (15), we derive (16), where the superscript (m, n, p, q) indicates association with the (m, n, p, q) -th messages. The underbraced parts, $a_{l,ui}^{(m,n,p,q)}$ and $a_{l,uj}^{(m,n,p,q)}$ denote the coefficients of the l -th parameter ($l = 0, 1, \dots, L-1$) in γ_{ui} and γ_{uj} , respectively. The final underbraced part, O_t , denotes the combined higher-order error. It is important to note that this error arises from the approximation inherent in the polynomial model. If the polynomial model can perfectly capture the variation of TDOA measurements over a short period, O_t can be neglected. In our study, we assume that the TDOA measurements can be accurately described by the polynomial model, which is a reasonable assumption supported by previous studies [28]. Therefore, we neglect the higher-order errors in subsequent illustrations.

We observe that the unknown variables $\gamma_{ui}^{(l)}$ and $\gamma_{uj}^{(l)}$ in (16) are TOA model parameters, which are unsolvable without two-way communication [28]. However, upon closer inspection of the part containing $\gamma_{ui}^{(l)}$ and $\gamma_{uj}^{(l)}$, it can be rewritten as

$$\begin{aligned} & a_{l,ui}^{(m,n,p,q)} \gamma_{ui}^{(l)} - a_{l,uj}^{(m,n,p,q)} \gamma_{uj}^{(l)} \\ & = a_{l,ui}^{(m,n,p,q)} (\gamma_{ui}^{(l)} - \gamma_{uj}^{(l)}) + (a_{l,ui}^{(m,n,p,q)} - a_{l,uj}^{(m,n,p,q)}) \gamma_{uj}^{(l)} \\ & = a_{l,ui}^{(m,n,p,q)} \gamma_{u;ij}^{(l)} + \Delta a_{l,u;ij}^{(m,n,p,q)} \gamma_{uj}^{(l)} \end{aligned} \quad (17)$$

where $\gamma_{u;ij}^{(l)} = \gamma_{ui}^{(l)} - \gamma_{uj}^{(l)}$ is the parameter of the TDOA model introduced in (8), and $\Delta a_{l,u;ij}^{(m,n,p,q)} = a_{l,ui}^{(m,n,p,q)} - a_{l,uj}^{(m,n,p,q)}$

is the difference of the parameter coefficients. The explicit expression for $\Delta a_{l,u;ij}^{(m,n,p,q)}$ is given by

$$\begin{aligned} \Delta a_{l,u;ij}^{(m,n,p,q)} & = (T_{ui}^{(m)l} - T_{uj}^{(n)l})(T_{ui}^{(p)} - T_{uj}^{(q)}) \\ & \quad - (T_{ui}^{(p)l} - T_{uj}^{(q)l})(T_{ui}^{(m)} - T_{uj}^{(n)}) \end{aligned} \quad (18)$$

If $\Delta a_{l,u;ij}^{(m,n,p,q)} = 0$ holds, $\gamma_{uj}^{(l)}$ is eliminated in (17), reducing (16) to an equation w.r.t. the TDOA model parameters $\gamma_{u;ij}$. By solving $\gamma_{u;ij}$, we can obtain the instantaneous TDOA estimates using (8).

We first discuss the universal approach for TDOA estimation when $\Delta a_{l,u;ij}^{(m,n,p,q)} = 0$ holds, and address the conditions under which this holds later. We substitute the noise-free timestamps and clock offsets in (16) with the actual measured timestamps and estimated clock offsets. Eventually, we obtain (19), where $\eta_{u;ij}^{(m,n,p,q)}$ is the combined noise, including the noise from timestamp measurements and clock offset estimation. Equation (19) is a linear equation with respect to $\gamma_{u;ij}$. It can be expressed as

$$b_{u;ij}^{(m,n,p,q)} = \mathbf{a}_{u;ij}^{(m,n,p,q)T} \gamma_{u;ij} + \eta_{u;ij}^{(m,n,p,q)} \quad (20)$$

where the expressions for $b_{u;ij}^{(m,n,p,q)}$, $\mathbf{a}_{u;ij}^{(m,n,p,q)}$ and $\eta_{u;ij}^{(m,n,p,q)}$ are provided in (21), (22) and (23), respectively.

Specifically, $a_{l,u;ij}^{(m,n,p,q)}$ is the coefficient of the l -th order TDOA parameter $\gamma_{u;ij}^{(l)}$, with its explicit form given in (19). Furthermore, the underbraced terms $\eta_{u;ij}^{(m,n,p,q)}$, $\eta_{u;ij}^{(m,n,p,q)(\phi)}$ and $\eta_{u;ij}^{(m,n,p,q)(w)}$ denote the noise contributions from clock offset of anchors, transmission timestamp measurements, and reception timestamp measurements, respectively. Suppose that we obtain M equations to solve for $\gamma_{u;ij} \in \mathbb{R}^{L \times 1}$. To ensure a unique solution, it is required that $M \geq L$. By combining the M equations, we formulate a system of linear equations,

$$\mathbf{b}_{u;ij} = \mathbf{A}_{u;ij} \gamma_{u;ij} + \boldsymbol{\eta}_{u;ij} \quad (24)$$

where

$$\mathbf{b}_{u;ij} = [b_{u;ij}^{(1)}, b_{u;ij}^{(2)}, \dots, b_{u;ij}^{(M)}]^T \quad (25)$$

$$\mathbf{A}_{u;ij} = [\mathbf{a}_{u;ij}^{(1)}, \mathbf{a}_{u;ij}^{(2)}, \dots, \mathbf{a}_{u;ij}^{(M)}]^T \quad (26)$$

$$\boldsymbol{\eta}_{u;ij} = [\eta_{u;ij}^{(1)}, \eta_{u;ij}^{(2)}, \dots, \eta_{u;ij}^{(M)}]^T \quad (27)$$

$$\begin{aligned}
& [(\hat{T}_i^{(m)} - \hat{\phi}_i^{(m)}) - (\hat{T}_j^{(n)} - \hat{\phi}_j^{(n)})](\hat{T}_{ui}^{(p)} - \hat{T}_{uj}^{(q)}) - [(\hat{T}_i^{(p)} - \hat{\phi}_i^{(p)}) - (\hat{T}_j^{(q)} - \hat{\phi}_j^{(q)})](\hat{T}_{ui}^{(m)} - \hat{T}_{uj}^{(n)}) + \\
& \sum_{l=0}^{L-1} \gamma_{u;ij}^{(l)} \underbrace{[\hat{T}_{ui}^{(m)l} (\hat{T}_{ui}^{(p)} - \hat{T}_{uj}^{(q)}) - \hat{T}_{ui}^{(p)l} (\hat{T}_{ui}^{(m)} - \hat{T}_{uj}^{(n)})]}_{a_{l,u;ij}^{(m,n,p,q)}} + \eta_{u;ij}^{(m,n,p,q)} = 0 \quad (19)
\end{aligned}$$

$$b_{u;ij}^{(m,n,p,q)} = -[(\hat{T}_i^{(m)} - \hat{\phi}_i^{(m)}) - (\hat{T}_j^{(n)} - \hat{\phi}_j^{(n)})](\hat{T}_{ui}^{(p)} - \hat{T}_{uj}^{(q)}) + [(\hat{T}_i^{(p)} - \hat{\phi}_i^{(p)}) - (\hat{T}_j^{(q)} - \hat{\phi}_j^{(q)})](\hat{T}_{ui}^{(m)} - \hat{T}_{uj}^{(n)}) \quad (21)$$

$$\mathbf{a}_{u;ij}^{(m,n,p,q)} = [a_{0,u;ij}^{(m,n,p,q)}, \dots, a_{l,u;ij}^{(m,n,p,q)}, \dots, a_{L-1,u;ij}^{(m,n,p,q)}]^T \quad (l = 0, 1, \dots, L-1) \quad (22)$$

$$\begin{aligned}
\eta_{u;ij}^{(m,n,p,q)} = & \underbrace{(\hat{T}_{ui}^{(p)} - \hat{T}_{uj}^{(q)})(\Delta\phi_i^{(m)} - \Delta\phi_j^{(n)}) - (\hat{T}_{ui}^{(m)} - \hat{T}_{uj}^{(n)})(\Delta\phi_i^{(p)} - \Delta\phi_j^{(q)})}_{\eta_{u;ij}^{(m,n,p,q)}(\phi)} + \\
& \underbrace{(\hat{T}_{ui}^{(m)} - \hat{T}_{uj}^{(n)})(v_i^{(p)} - v_j^{(q)}) - (\hat{T}_{ui}^{(p)} - \hat{T}_{uj}^{(q)})(v_i^{(m)} - v_j^{(n)})}_{\eta_{u;ij}^{(m,n,p,q)}(v)} + \\
& \underbrace{[(\hat{T}_i^{(p)} - \hat{\phi}_i^{(p)}) - (\hat{T}_j^{(q)} - \hat{\phi}_j^{(q)})](w_{ui}^{(m)} - w_{uj}^{(n)}) - [(\hat{T}_i^{(m)} - \hat{\phi}_i^{(m)}) - (\hat{T}_j^{(n)} - \hat{\phi}_j^{(n)})](w_{ui}^{(p)} - w_{uj}^{(q)})}_{\eta_{u;ij}^{(m,n,p,q)}(w)} \quad (23)
\end{aligned}$$

The superscripts of $b_{u;ij}$, $a_{u;ij}$, and $\eta_{u;ij}$ represent the equation indices. The solution to (24) is obtained in a WLS sense as

$$\hat{\gamma}_{u;ij} = (\mathbf{A}_{u;ij}^T \Sigma_{\eta_{u;ij}}^{-1} \mathbf{A}_{u;ij})^{-1} \mathbf{A}_{u;ij}^T \Sigma_{\eta_{u;ij}}^{-1} \mathbf{b}_{u;ij} \quad (28)$$

$$\Sigma_{\gamma_{u;ij}} = (\mathbf{A}_{u;ij}^T \Sigma_{\eta_{u;ij}}^{-1} \mathbf{A}_{u;ij})^{-1} \quad (29)$$

where $\Sigma_{\eta_{u;ij}}$ denotes the covariance matrix of $\eta_{u;ij}$ and $\Sigma_{\gamma_{u;ij}}$ denotes the covariance matrix of the estimated parameter vector $\hat{\gamma}_{u;ij}$. The matrix $\Sigma_{\eta_{u;ij}}$ is determined by the TD protocol and the specific equation construction method used. In Section IV-B, we provide a specific example for our problem setting.

After obtaining $\hat{\gamma}_{u;ij}$, the instantaneous TDOA estimate $\tau_{u;ij}$ at t_u can be estimated by (8) as

$$\hat{\tau}_{u;ij}(t_u) = \boldsymbol{\nu}_{t_u}^T \hat{\gamma}_{u;ij} \quad (30)$$

and the variance of the estimate $\hat{\tau}_{u;ij}$ is given by

$$\sigma_{\tau_{u;ij}}^2 = \boldsymbol{\nu}_{t_u}^T \Sigma_{\gamma_{u;ij}} \boldsymbol{\nu}_{t_u} \quad (31)$$

To summarize, we employ WLS to estimate the parameters of the TDOA model. Neglecting higher-order errors, $\eta_{u;ij}$ can be regarded as a zero-mean noise vector, which implies that the derived model parameter estimates and instantaneous TDOA estimates are unbiased. Since this algorithm is designed for mobile targets, we refer to it as Mobile Weighted Least Squares.

2) *Successive Time Difference Strategy*: The aforementioned algorithm assumes that condition $\Delta a_{l,u;ij}^{(m,n,p,q)} = 0$ is met. Here, we discuss the scenarios under which this condition is valid. It is evident from (18) that $\Delta a_{l,u;ij}^{(m,n,p,q)} = 0$ holds when $l = 0, 1$. For higher-order cases, i.e. $l \geq 2$, we find that $\Delta a_{l,u;ij}^{(m,n,p,q)} \neq 0$ inherently.

A special case exists for $l = 2$, where $\Delta a_{2,u;ij}^{(m,n,p,q)}$ is given by

$$\Delta a_{2,u;ij}^{(m,n,p,q)} = (T_{ui}^{(m)} - T_{uj}^{(n)})(T_{ui}^{(p)} - T_{uj}^{(q)})(T_{ui}^{(m)} + T_{uj}^{(n)} - T_{ui}^{(p)} - T_{uj}^{(q)}) \quad (32)$$

If we assign $m = q = s$, $n = p = s + 1$ ($s \in \mathbb{N}^+$) and assume that the transmission intervals of Anchor i and Anchor j and the corresponding reception intervals of two successive signals are identical or extremely close, i.e.,

$$\Delta T_{ij} \approx T_{ui}^{(s)} - T_{uj}^{(s)} \approx T_{ui}^{(s+1)} - T_{uj}^{(s+1)} \quad (33)$$

It turns out that

$$T_{ui}^{(m)} + T_{uj}^{(n)} - T_{ui}^{(p)} - T_{uj}^{(q)} = (T_{ui}^{(s)} - T_{uj}^{(s)}) - (T_{ui}^{(s+1)} - T_{uj}^{(s+1)}) \approx 0 \quad (34)$$

which consequently results in $\Delta a_{2,u;ij}^{(m,n,p,q)} \approx 0$. Fortunately, the condition (33) holds for the TD protocol in our problem setting, and this condition can serve as a guideline for the design of the measurement protocol if other protocols are adopted.

With the above assumptions, if we revisit equations (12) and (13), we notice a departure from the existing TDOA estimation methods. In conventional methods, TOAs from two anchors are typically selected at the same time (or nearly the same time) to compute differences. However, in our approach,

we construct equations using TOAs from two anchors at different but successive frames. This strategy of time differences may seem counterintuitive but is fundamental to our P-TDOA method, which we call the Successive Time Difference Strategy. On the one hand, STDS ensures $\Delta a_{2,u;ij}^{(m,n,p,q)} \approx 0$, allowing the TDOA model to be extended to higher orders. On the other hand, STDS prevents the problem from becoming ill-posed. For instance, if we use TOAs within the same frame for differencing, i.e., $m = n = s$, $p = q = s + 1$, which is closer to traditional TDOA estimation methods like A-TDOA [19].

$\Delta a_{l,u;ij}^{m,n,p,q} = 0$ still holds for $l = 0, 1$, and the corresponding coefficients become

$$\begin{aligned} a_{0,u;ij}^{(s)} &= (T_{ui}^{(s+1)} - T_{uj}^{(s+1)}) - (T_{ui}^{(s)} - T_{uj}^{(s)}) \approx 0 \\ a_{1,u;ij}^{(s)} &= T_{ui}^{(s)}(T_{ui}^{(s+1)} - T_{uj}^{(s+1)}) - T_{ui}^{(s+1)}(T_{ui}^{(s)} - T_{uj}^{(s)}) \\ &= (T_{ui}^{(s)} - T_{ui}^{(s+1)})\Delta T_{ij} \end{aligned} \quad (35)$$

Under our TD protocol introduced in Section II-B, $T_{ui}^{(s)} - T_{uj}^{(s+1)} = -T_f$ and $\Delta T_{ij} = (i - j)T_s$, where T_f and T_s are the duration of one frame and one slot, respectively. In this way, $a_{0,u;ij}^{(s)} \approx 0$ and $a_{1,u;ij}^{(s)}$ is approximately constant for all $s \in \mathbb{N}^+$. Consequently, two columns of the coefficient matrix $\mathbf{A}_{u;ij}$ are nearly fully correlated in (26), rendering $\mathbf{A}_{u;ij}$ rank-deficient, and thus making the problem unsolvable. In contrast, STDS ensures that the coefficient matrix $\mathbf{A}_{u;ij}$ is full-rank, resulting in a unique solution.

In certain special instances, the difference of the l -th parameter coefficients, $\Delta a_{l,u;ij}^{(m,n,p,q)}$, may still be equal to zero when $l > 2$, but this is not generally applicable. In most scenarios, the number of model parameters $L = 3$, corresponding to the second order model, is sufficient to describe the nonlinearity of time-varying TDOAs over short periods, as validated by our subsequent simulation experiments. Therefore, in our later discussions, we focus on cases where $L \leq 3$ and $\Delta a_{l,u;ij}^{(m,n,p,q)} = 0$ can be strictly or approximately satisfied.

C. Mobile Target Localization

Given the TDOAs between a target and multiple pairs of stationary anchors with known positions, the position of the target can be determined by solving a set of hyperbolic equations. Each hyperbolic equation represents a hyperbolic curve with the foci located at the positions of the respective anchor pairs. Numerous algorithms have been proposed to solve this problem [26], [27], [32], [33]. However, these methods rely on the fundamental assumption that the TDOAs correspond to the same target position. In dynamic scenarios, this means requiring instantaneous TDOAs from multiple anchor pairs at the same time, which is not feasible with traditional methods, as signals from different anchors do not arrive at the target simultaneously.

Fortunately, P-TDOA has overcome this challenge and can obtain TDOAs of different anchor pairs at the same time. For instance, suppose we have obtained $\gamma_{u;ij}(i, j \in \mathcal{N}_a, i < j)$ and we want to determine Target u 's position at t_u . By substituting $\hat{\gamma}_{u;ij}$ and t_u into (8), we can obtain $\hat{\tau}_{u;ij}(t_u)$ and the set of TDOAs is denoted as $\hat{\tau}_u(t_u)$. Subsequently, with the instantaneous TDOAs $\hat{\tau}_u(t_u)$ and known positions of anchors, we can localize Target u using classical TDOA-based multilateration methods. We select the algorithm in [27] as the basis for our mobile target localization algorithm, which provides a closed-form solution and approximates the ML estimator under small noise conditions, while accounting for uncertainties in the anchors' positions. For further details of the multilateration algorithm, readers are referred to [27]. The procedure of our proposed mobile target localization method based on P-TDOA is summarized in Algorithm 1.

Algorithm 1 Mobile Target Localization based on P-TDOA

- 1: **Input:** Measurements and information of Anchor i and Target u in N_f frames, $i \in \mathcal{N}_a$
 - 2: (1) The recorded timestamps,
 - 3: $\hat{\mathbf{t}}_i = [\hat{T}_i^{(1)}, \hat{T}_i^{(2)}, \dots, \hat{T}_i^{(N_f)}]^T$
 - 4: $\hat{\mathbf{t}}_{ui} = [\hat{T}_{ui}^{(1)}, \hat{T}_{ui}^{(2)}, \dots, \hat{T}_{ui}^{(N_f)}]^T$
 - 5: (2) The estimated clock offsets $[\hat{\phi}_i^{(1)}, \hat{\phi}_i^{(2)}, \dots, \hat{\phi}_i^{(N_f)}]$ with their standard deviations $[\sigma_{\phi_i^{(1)}}, \sigma_{\phi_i^{(2)}}, \dots, \sigma_{\phi_i^{(N_f)}}]^T$ of anchors
 - 6: (3) The positions with uncertainty of anchors $(\hat{\mathbf{p}}_i, \Sigma_{\mathbf{p}_i})$
 - 7: **Output:** The position estimate $\hat{\mathbf{p}}_u(t_u)$ of Target u at t_u
 - 8: **Procedure:**
 - 9: **for** $n = 1$ to N_p **do**
 - 10: Obtain the anchor index of n -th anchor pair $(i, j) = [\mathcal{N}_p]_n$
 - 11: Estimate $\hat{\gamma}_{u;ij}$ and $\Sigma_{\gamma_{u;ij}}$ using (26)-(31)
 - 12: Calculate the instantaneous TDOA estimate $\hat{\tau}_{u;ij}$ and its variance $\sigma_{\tau_{u;ij}}^2$ at t_u based on (32) and (33)
 - 13: **end for**
 - 14: Select one reference anchor such as Anchor 1 and combine the TDOAs with variances linked to the reference anchor as $\hat{\tau}_u(t_u) = [\hat{\tau}_{u;21}, \hat{\tau}_{u;31}, \dots, \hat{\tau}_{u;N_a 1}]^T$ and $\Sigma_{\tau_u} = \text{diag}([\sigma_{\tau_{u;12}}^2, \sigma_{\tau_{u;13}}^2, \dots, \sigma_{\tau_{u;1N_a}}^2]^T)$
 - 15: Solve the position $\hat{\mathbf{p}}_u(t_u)$ by the algorithm in [27]
-

IV. PERFORMANCE ANALYSIS

A. Cramér-Rao Lower Bound

In this section, we analyze the CRLBs for instantaneous TDOA estimation and localization of a mobile target, using them as theoretical lower bounds for performance comparison. However, sequential TOA measurements are not suitable for analyzing CRLB for instantaneous TDOA estimation because they are obtained at different times. Similarly, they cannot be used to analyze the CRLB for localization without incorporating motion modeling, as they do not correspond to the same position of the target [22]–[24]. Therefore, we analyze the case of concurrent TOA measurements, where the target receives signals from multiple anchors simultaneously. It is important to note that while the concurrent TOA measurements can only be obtained in frequency-division (FD) or code-division (CD) systems, such as GNSS, they cannot be obtained in practical TD systems. The CRLBs derived here represent theoretical limits that are challenging to reach for sequential measurements, serving as a reference lower bound for analysis.

1) *CRLB for instantaneous TDOA estimation:* For deriving the CRLB for instantaneous TDOA estimation in concurrent TOA scenarios, we make the following assumptions. First, Target u receives signals simultaneously from multiple anchors at the start of each frame. Additionally, the noise considered includes both the timestamp measurement noise and the clock offsets of the anchors.

We take anchor pair (i, j) and Frame m for example. The notations are consistent with those used earlier in the text. As the reception times are quite close, we assume that the clock offset of Target u remains the same, denoted as $\phi_u^{(m)}$.

Considering the clock offsets of the anchors and the target, the TOA equations can be written as

$$\begin{aligned} T_i^{(m)} - \phi_i^{(m)} + \tau_{ui}^{(m)} &= T_{ui}^{(m)} - \phi_u^{(m)} \\ T_j^{(m)} - \phi_j^{(m)} + \tau_{uj}^{(m)} &= T_{uj}^{(m)} - \phi_u^{(m)} \end{aligned} \quad (36)$$

Thus, the instantaneous TDOA in Frame m can be expressed as

$$\begin{aligned} \tau_{u;ij}^{(m)} &= \tau_{ui}^{(m)} - \tau_{uj}^{(m)} \\ &= (T_{ui}^{(m)} - T_i^{(m)}) - (T_{uj}^{(m)} - T_j^{(m)}) + (\phi_i^{(m)} - \phi_j^{(m)}) \end{aligned} \quad (37)$$

We incorporate the noise of timestamps and clock offset errors of the anchors to derive the actual instantaneous TDOA measurement as follows:

$$\begin{aligned} \hat{\tau}_{u;ij}^{(m)} &= (\hat{T}_{ui}^{(m)} - \hat{T}_i^{(m)}) - (\hat{T}_{uj}^{(m)} - \hat{T}_j^{(m)}) + (\hat{\phi}_i^{(m)} - \hat{\phi}_j^{(m)}) + \\ &\quad (v_i^{(m)} - v_j^{(m)}) - (w_{ui}^{(m)} - w_{uj}^{(m)}) - (\Delta\phi_i^{(m)} - \Delta\phi_j^{(m)}) \\ &= \tau_{u;ij}^{(m)} + \Delta\tau_{u;ij}^{(m)} \end{aligned} \quad (38)$$

where $\Delta\tau_{u;ij}^{(m)} = (v_i^{(m)} - v_j^{(m)}) - (w_{ui}^{(m)} - w_{uj}^{(m)}) - (\Delta\phi_i^{(m)} - \Delta\phi_j^{(m)})$ represents the error in the instantaneous TDOA estimate $\hat{\tau}_{u;ij}^{(m)}$.

Considering the noise in the recorded timestamps and errors in the anchors' clock offsets, the errors in the instantaneous TDOA measurements are the combined effects of the noise from two TOA measurements. We assume that the noise in the transmission timestamps, reception timestamps, and clock offsets of the anchors are independent and identically distributed Gaussian white noise with different variances, respectively, i.e., $w \sim \mathcal{N}(0, \sigma_w^2)$, $v \sim \mathcal{N}(0, \sigma_v^2)$ and $\phi \sim \mathcal{N}(0, \sigma_\phi^2)$. In this way, $\Delta\tau_{u;ij}^{(m)} \sim \mathcal{N}(0, 2(\sigma_v^2 + \sigma_w^2 + \sigma_\phi^2))$, and we denote $\sigma_n^2 = 2(\sigma_w^2 + \sigma_v^2 + \sigma_\phi^2)$ as the variance of an independent instantaneous TDOA measurement, i.e., $\Delta\tau_{u;ij}^{(m)} \sim \mathcal{N}(0, \sigma_n^2)$.

Assume that Target u obtains N_f instantaneous TDOA measurements from Anchor i and j denoted as $\hat{\tau}_{u;ij} = [\hat{\tau}_{u;ij}^{(1)}, \hat{\tau}_{u;ij}^{(2)}, \dots, \hat{\tau}_{u;ij}^{(N_f)}]^T$ at $\mathbf{t}_u = [t_u^{(1)}, t_u^{(2)}, \dots, t_u^{(N_f)}]^T$. The covariance matrix of $\hat{\tau}_{u;ij}$ is $\Sigma_{\tau_{u;ij}} = \sigma_n^2 \mathbf{I}_{N_f}$, which also represents the CRLB of instantaneous TDOA estimation, denoted as

$$\text{CRLB1} = \sigma_n^2 \mathbf{I}_{N_f} \quad (39)$$

However, since we apply a polynomial model to the TDOA measurements in our method, as in (8), which effectively adds constraints on the measurements, we must consider the impact of the TDOA model. Revisiting (8), the N_f instantaneous TDOA estimates at \mathbf{t}_u can be written as

$$\begin{aligned} \boldsymbol{\tau}_{u;ij} &= [\boldsymbol{\nu}_{t_u^{(1)}}^T \boldsymbol{\gamma}_{u;ij}, \boldsymbol{\nu}_{t_u^{(2)}}^T \boldsymbol{\gamma}_{u;ij}, \dots, \boldsymbol{\nu}_{t_u^{(N_f)}}^T \boldsymbol{\gamma}_{u;ij}]^T \\ &= [\boldsymbol{\nu}_{t_u^{(1)}}, \boldsymbol{\nu}_{t_u^{(2)}}, \dots, \boldsymbol{\nu}_{t_u^{(N_f)}}]^T \boldsymbol{\gamma}_{u;ij} \\ &= [\mathbf{t}_u^{\odot 0}, \mathbf{t}_u^{\odot 1}, \dots, \mathbf{t}_u^{\odot L-1}] \boldsymbol{\gamma}_{u;ij} \\ &= \mathbf{V}_u \boldsymbol{\gamma}_{u;ij} \end{aligned} \quad (40)$$

where $\mathbf{V}_u \in \mathbb{R}^{N_f \times L}$ is defined as

$$\mathbf{V}_u = \mathcal{V}(\mathbf{t}_u) = [\mathbf{t}_u^{\odot 0}, \mathbf{t}_u^{\odot 1}, \dots, \mathbf{t}_u^{\odot L-1}] \quad (41)$$

Here, \mathcal{V} represents an operator that transform a vector into a transpose of a Vandermonde matrix. Although \mathbf{V}_u may be non-invertible, however, the Vandermonde matrix \mathbf{V}_u is guaranteed to have full column rank if $N_f \geq L$. In this case, the matrix \mathbf{V}_u has a unique left inverse, denoted as \mathbf{V}_u^\dagger [34], given by

$$\mathbf{V}_u^\dagger = (\mathbf{V}_u^T \mathbf{V}_u)^{-1} \mathbf{V}_u^T \quad (42)$$

We use \mathbf{V}_u^\dagger to rewrite the relationship in (40) by

$$\boldsymbol{\gamma}_{u;ij} = \mathbf{V}_u^\dagger \boldsymbol{\tau}_{u;ij} \quad (43)$$

The CRLB of $\boldsymbol{\gamma}_{u;ij}$ is derived as follows [35]:

$$\begin{aligned} \text{CRLB}(\boldsymbol{\gamma}_{u;ij}) &= \frac{\partial \boldsymbol{\gamma}_{u;ij}}{\partial \boldsymbol{\tau}_{u;ij}} \text{CRLB}(\boldsymbol{\tau}_{u;ij}) \frac{\partial \boldsymbol{\gamma}_{u;ij}}{\partial \boldsymbol{\tau}_{u;ij}}^T \\ &= \mathbf{V}_u^\dagger (\sigma_n^2 \mathbf{I}_{N_f}) \mathbf{V}_u^\dagger{}^T = \sigma_n^2 (\mathbf{V}_u^T \mathbf{V}_u)^{-1} \end{aligned} \quad (44)$$

The CRLB for the instantaneous TDOA estimates $\boldsymbol{\tau}_{u;ij}$ under the polynomial model can then be calculated as follows:

$$\begin{aligned} \text{CRLB2}(\boldsymbol{\tau}_{u;ij}) &= \mathbf{V}_u^T \text{CRLB}(\boldsymbol{\gamma}_{u;ij}) \mathbf{V}_u \\ &= \sigma_n^2 \mathbf{V}_u (\mathbf{V}_u^T \mathbf{V}_u)^{-1} \mathbf{V}_u^T \end{aligned} \quad (45)$$

We use CRLB1 and CRLB2 to distinguish between the CRLB for instantaneous TDOA estimation without and with the polynomial TDOA model. The same distinction applies to the CRLB for localization as well.

2) *CRLB for localization*: Regarding the CRLB for localization of a mobile target, we also consider the scenario of concurrent TOA measurements. The CRLB for localization has been demonstrated in [26], [27], given a vector of TDOA measurements with a covariance matrix \mathbf{Q} . We will not repeat the derivation here. However, it is important to note that the CRLB for localization is influenced by the covariance matrix of the TDOA estimates. Whether or not the polynomial TDOA model is applied during TDOA estimation will impact the covariance matrix of the TDOA estimates, thereby affecting the CRLB for localization.

If the polynomial TDOA model is not applied, the CRLB for localization across different frames remains identical, as the covariance matrix of the TDOA estimates, denoted as \mathbf{Q}_u , remains unchanged⁴

$$\mathbf{Q}_u = \frac{1}{2} \begin{bmatrix} 2\sigma_n^2 & \sigma_n^2 & \dots & \sigma_n^2 \\ \sigma_n^2 & 2\sigma_n^2 & \dots & \sigma_n^2 \\ \vdots & \vdots & \ddots & \sigma_n^2 \\ \sigma_n^2 & \sigma_n^2 & \dots & 2\sigma_n^2 \end{bmatrix} \quad (46)$$

However, if the polynomial TDOA model is applied, the covariance matrix of the TDOA estimates may vary across different frames. We collect the diagonal entries of $\text{CRLB2}(\boldsymbol{\tau}_{u;ij})$ as

$$\begin{aligned} \boldsymbol{\lambda}_n &= \text{diag} \left(\sigma_n^2 \mathbf{V}_u (\mathbf{V}_u^T \mathbf{V}_u)^{-1} \mathbf{V}_u^T \right) \\ &= [\sigma_n^{(1)2}, \sigma_n^{(2)2}, \dots, \sigma_n^{(N_f)2}] \end{aligned} \quad (47)$$

⁴Here we also follow the method in [27] and select Anchor 1 as the reference anchor. All the TDOA estimates are between Target u and anchor pair (1,i) ($i \in \mathcal{N}_a, i \neq 1$)

In this way, the covariance matrix of TDOA estimates of Frame m can be written as

$$\mathbf{Q}_u^{(m)} = \frac{1}{2} \begin{bmatrix} 2\sigma_n^{(m)2} & \sigma_n^{(m)2} & \cdots & \sigma_n^{(m)2} \\ \sigma_n^{(m)2} & 2\sigma_n^{(m)2} & \cdots & \sigma_n^{(m)2} \\ \vdots & \vdots & \ddots & \sigma_n^{(m)2} \\ \sigma_n^{(m)2} & \sigma_n^{(m)2} & \cdots & 2\sigma_n^{(m)2} \end{bmatrix} \quad (48)$$

where $m = 1, 2, \dots, N_f$. Using the newly derived covariance matrix of the TDOA measurements, we can determine the CRLB for localization in the corresponding frames.

B. Theoretical MSE

1) *MSE for instantaneous TDOA estimation*: We have derived the covariance expressions for the estimated parameters, $\hat{\gamma}_{u;ij}$ and the estimated TDOA, $\hat{\tau}_{u;ij}$, in (29) and (31), respectively. However, these expressions contain the unspecified term, $\Sigma_{\eta_{u;ij}}$. To evaluate the performance of the proposed P-TDOA, we analyze the theoretical MSE of $\hat{\gamma}_{u;ij}$ and $\hat{\tau}_{u;ij}$ using the STDS under our periodic broadcast TD protocol.

Target u can receive one signal from each anchor in a single frame. With STDS, the information from two successive frames is used to formulate one equation. Therefore, at least N_f frames to obtain $N_f - 1$ independent equations in (24).

The vector of errors for the anchors' clock offset estimates, along with the noise in the transmission and reception timestamps over N_f frames, is denoted as

$$\begin{aligned} \Delta\phi_i &= [\Delta\phi_i^{(1)}, \dots, \Delta\phi_i^{(N_f)}], & \Delta\phi_j &= [\Delta\phi_j^{(1)}, \dots, \Delta\phi_j^{(N_f)}] \\ \mathbf{v}_i &= [v_i^{(1)}, \dots, v_i^{(N_f)}], & \mathbf{v}_j &= [v_j^{(1)}, \dots, v_j^{(N_f)}] \\ \mathbf{w}_{ui} &= [w_{ui}^{(1)}, \dots, w_{ui}^{(N_f)}], & \mathbf{w}_{uj} &= [w_{uj}^{(1)}, \dots, w_{uj}^{(N_f)}] \end{aligned} \quad (49)$$

The combined noise in (27) can then be specified by

$$\begin{aligned} \eta_{u;ij} &= \mathbf{C}_{u;ij}^{\phi_i} \Delta\phi_i + \mathbf{C}_{u;ij}^{\phi_j} \Delta\phi_j + \mathbf{C}_{u;ij}^{\mathbf{v}_i} \mathbf{v}_i + \\ & \mathbf{C}_{u;ij}^{\mathbf{v}_j} \mathbf{v}_j + \mathbf{C}_{u;ij}^{\mathbf{w}_{ui}} \mathbf{w}_{ui} + \mathbf{C}_{u;ij}^{\mathbf{w}_{uj}} \mathbf{w}_{uj} \end{aligned} \quad (50)$$

where the entries in $\mathbf{C}_{u;ij}^{\phi_i}$, $\mathbf{C}_{u;ij}^{\phi_j}$, $\mathbf{C}_{u;ij}^{\mathbf{v}_i}$, $\mathbf{C}_{u;ij}^{\mathbf{v}_j}$, $\mathbf{C}_{u;ij}^{\mathbf{w}_{ui}}$, $\mathbf{C}_{u;ij}^{\mathbf{w}_{uj}}$ are all zero except for the following items:

$$\begin{aligned} [\mathbf{C}_{u;ij}^{\phi_i}]_{s,s:s+1} &= [(\hat{T}_{ui}^{(s+1)} - \hat{T}_{uj}^{(s)}), -(\hat{T}_{ui}^{(s)} - \hat{T}_{uj}^{(s+1)})] \\ [\mathbf{C}_{u;ij}^{\phi_j}]_{s,s:s+1} &= [(\hat{T}_{ui}^{(s)} - \hat{T}_{uj}^{(s+1)}), -(\hat{T}_{ui}^{(s+1)} - \hat{T}_{uj}^{(s)})] \\ [\mathbf{C}_{u;ij}^{\mathbf{v}_i}]_{s,s:s+1} &= [-(\hat{T}_{ui}^{(s+1)} - \hat{T}_{uj}^{(s)}), (\hat{T}_{ui}^{(s)} - \hat{T}_{uj}^{(s+1)})] \\ [\mathbf{C}_{u;ij}^{\mathbf{v}_j}]_{s,s:s+1} &= [-(\hat{T}_{ui}^{(s)} - \hat{T}_{uj}^{(s+1)}), (\hat{T}_{ui}^{(s+1)} - \hat{T}_{uj}^{(s)})] \\ [\mathbf{C}_{u;ij}^{\mathbf{w}_{ui}}]_{s,s} &= [(\hat{T}_i^{(s+1)} - \hat{\phi}_i^{(s+1)}) - (\hat{T}_j^{(s)} - \hat{\phi}_j^{(s)})] \\ [\mathbf{C}_{u;ij}^{\mathbf{w}_{ui}}]_{s,s+1} &= [(\hat{T}_j^{(s+1)} - \hat{\phi}_j^{(s+1)}) - (\hat{T}_i^{(s)} - \hat{\phi}_i^{(s)})] \\ [\mathbf{C}_{u;ij}^{\mathbf{w}_{uj}}]_{s,s} &= [(\hat{T}_i^{(s)} - \hat{\phi}_i^{(s)}) - (\hat{T}_j^{(s+1)} - \hat{\phi}_j^{(s+1)})] \\ [\mathbf{C}_{u;ij}^{\mathbf{w}_{uj}}]_{s,s+1} &= [(\hat{T}_j^{(s)} - \hat{\phi}_j^{(s)}) - (\hat{T}_i^{(s+1)} - \hat{\phi}_i^{(s+1)})] \end{aligned} \quad (51)$$

where $s = 1, 2, \dots, N_f - 1$. Thus, the covariance matrix of $\eta_{u;ij}$ can be calculated by:

$$\begin{aligned} \Sigma_{\eta_{u;ij}} &= \mathbf{E} \{ \eta_{u;ij} \eta_{u;ij}^T \} \\ &= \mathbf{C}_{u;ij}^{\phi_i} \Sigma_{\phi_i} \mathbf{C}_{u;ij}^{\phi_i T} + \mathbf{C}_{u;ij}^{\mathbf{v}_i} \Sigma_{\mathbf{v}_i} \mathbf{C}_{u;ij}^{\mathbf{v}_i T} + \mathbf{C}_{u;ij}^{\mathbf{w}_{ui}} \Sigma_{\mathbf{w}_{ui}} \mathbf{C}_{u;ij}^{\mathbf{w}_{ui} T} \\ & \quad + \mathbf{C}_{u;ij}^{\phi_j} \Sigma_{\phi_j} \mathbf{C}_{u;ij}^{\phi_j T} + \mathbf{C}_{u;ij}^{\mathbf{v}_j} \Sigma_{\mathbf{v}_j} \mathbf{C}_{u;ij}^{\mathbf{v}_j T} + \mathbf{C}_{u;ij}^{\mathbf{w}_{uj}} \Sigma_{\mathbf{w}_{uj}} \mathbf{C}_{u;ij}^{\mathbf{w}_{uj} T} \end{aligned} \quad (52)$$

Additionally, with the TD protocol and STDS applied, the coefficients matrix $\mathbf{A}_{u;ij}$ in (26) can be specified as well, where the entries are all zero except for the following items:

$$\begin{aligned} [\mathbf{A}_{u;ij}]_{s,l} &= (\hat{T}_{ui}^{(s)})^{l-1} (\hat{T}_{ui}^{(s+1)} - \hat{T}_{uj}^{(s)}) - \\ & (\hat{T}_{ui}^{(s+1)})^{l-1} (\hat{T}_{ui}^{(s)} - \hat{T}_{uj}^{(s+1)}) \end{aligned} \quad (53)$$

where $s = 1, 2, \dots, N_f - 1$ and $l = 0, 1, \dots, L - 1$.

To simplify the analysis, we make some approximations to the aforementioned matrices. By neglecting the extremely short propagation time, it approximately holds that:

$$\begin{aligned} \hat{T}_i^{(m)} - \hat{\phi}_i^{(m)} &\approx \hat{T}_{ui}^{(m)} \\ \hat{T}_{ui}^{(m)} - \hat{T}_{uj}^{(n)} &\approx (m - n)T_f + (i - j)T_s \end{aligned} \quad (54)$$

Then $\Sigma_{\eta_{u;ij}}$ and $\mathbf{A}_{u;ij}$ can be rewritten as

$$\Sigma_{\eta_{u;ij}} = \sigma_n^2 \begin{bmatrix} (r_1^2 + r_2^2) & r_1 r_2 & \cdots & 0 \\ r_1 r_2 & (r_1^2 + r_2^2) & \cdots & \vdots \\ \vdots & \vdots & \ddots & r_1 r_2 \\ 0 & \cdots & r_1 r_2 & (r_1^2 + r_2^2) \end{bmatrix} \quad (55)$$

$$\mathbf{A}_{u;ij} = \mathbf{B}\mathcal{V}(\mathbf{t}_{ui}) = \mathbf{B}\mathbf{V}_i \quad (56)$$

where r_1 and r_2 satisfy

$$\begin{aligned} r_1 &= T_f + (i - j)T_s \\ r_2 &= T_f - (i - j)T_s \end{aligned} \quad (57)$$

The operator \mathcal{V} is defined in (41), and $\mathbf{t}_{ui} = [T_{ui}^{(1)}, \dots, T_{ui}^{(N_f)}]$ is the vector of Target u 's reception times of signals from Anchor i . The matrix \mathbf{B} satisfies

$$\mathbf{B} = \begin{bmatrix} r_1 & r_2 & 0 & \cdots & 0 & 0 \\ 0 & r_1 & r_2 & \cdots & 0 & 0 \\ \vdots & \vdots & \vdots & \ddots & \vdots & \\ 0 & 0 & 0 & \cdots & r_1 & r_2 \end{bmatrix} \quad (58)$$

By substituting (55) and (56) into (29) we obtain

$$\Sigma_{\gamma_{u;ij}} = [\mathbf{V}_i^T (\mathbf{B}^T \Sigma_{\eta_{u;ij}}^{-1} \mathbf{B}) \mathbf{V}_i]^{-1} \quad (59)$$

Let's consider $\mathbf{D} = \mathbf{B}^T \Sigma_{\eta_{u;ij}}^{-1} \mathbf{B} \cdot \sigma_n^2$. Since the inverse of the symmetric triple diagonal matrix in (55) has no straightforward analytical solution, simplifying \mathbf{D} becomes challenging.

Therefore, we proceed by considering a special case where $T_f \gg |i - j| T_s$. Then \mathbf{D} can be approximated as

$$\begin{aligned} \mathbf{D} &= \begin{bmatrix} \frac{N_f-1}{N_f} & \frac{1}{N_f} & \cdots & (-1)^{N_f} \frac{1}{N_f} \\ \frac{1}{N_f} & \frac{N_f-1}{N_f} & \cdots & (-1)^{N_f+1} \frac{1}{N_f} \\ \vdots & \vdots & \ddots & \vdots \\ (-1)^L \frac{1}{N_f} & (-1)^{L+1} \frac{1}{N_f} & \cdots & (-1)^{N_f+L-1} \frac{1}{N_f} \end{bmatrix} \\ &= \mathbf{I}_{N_f} + \frac{1}{N_f} \begin{bmatrix} -1 & 1 & \cdots & (-1)^{N_f} \\ 1 & -1 & \cdots & (-1)^{N_f+1} \\ \vdots & \vdots & \ddots & \vdots \\ (-1)^{N_f} & (-1)^{N_f+1} & \cdots & (-1)^{2N_f-1} \end{bmatrix} \\ &= \mathbf{I}_{N_f} + \Delta \mathbf{D} \end{aligned} \quad (60)$$

If we consider the instantaneous TDOA measurements at the instants when Anchor i transmits, i.e. $\mathbf{t}_u = \mathbf{t}_{ui}$ and $\mathbf{V}_u = \mathbf{V}_i$, we denote $\mathbf{F} = \mathbf{V}_u^T \mathbf{D} \mathbf{V}_u = (\mathbf{V}_u^T \mathbf{V}_u) + (\mathbf{V}_u^T \Delta \mathbf{D} \mathbf{V}_u) = \mathbf{F}_1 + \mathbf{F}_2$. The entries at the i -th row and j -th column of \mathbf{F}_1 and \mathbf{F}_2 can be calculated as

$$\begin{aligned} [\mathbf{F}_1]_{i,j} &= \sum_{n=1}^{N_f} t_u^{(n)i-1} t_u^{(n)j-1} \\ [\mathbf{F}_2]_{i,j} &= \frac{1}{N_f} \left[\sum_{n=1}^{N_f} t_u^{(n)i-1} (-1)^n \right] \left[\sum_{n=1}^{N_f} t_u^{(n)j-1} (-1)^{n-1} \right] \end{aligned} \quad (61)$$

It is observed that $[\mathbf{F}_1]_{i,j} \gg [\mathbf{F}_2]_{i,j}$, and this holds more strictly as N_f increases. If \mathbf{F}_2 can be neglected compared to \mathbf{F}_1 , then (58) reduces to

$$\Sigma_{\gamma_{u;ij}} = \sigma_n^2 (\mathbf{V}_u^T \mathbf{V}_u)^{-1} = \text{CRLB}(\gamma_{u;ij}) \quad (62)$$

where $\text{CRLB}(\gamma_{u;ij})$ is derived in (44). Consequently, the MSE of instantaneous TDOA estimation can also reach the CRLB.

To summarize, the conditions for the theoretical MSE of instantaneous TDOA estimation to reach the CRLB are as follows⁵:

- The transmission intervals between anchors are relatively small compared to the frame length.
- $[\mathbf{F}_1]_{i,j} \gg [\mathbf{F}_2]_{i,j}$, which is generally satisfied if N_f is sufficiently large.

We can interpret the two conditions as follows. Since concurrent TOA measurements are not available in a TDBPS, we can only use sequential TOA measurements to approximate the results. If $T_f \geq |i - j| T_s$, meaning that the transmission interval between Anchor i and Anchor j within the same frame is small compared to the transmission interval of one anchor across two successive frames, the signals from Anchor i and Anchor j can be viewed as transmitted almost simultaneously, approximating the scenario of concurrent TOA measurements. Moreover, estimating the parameters of polynomial models resembles a fitting process, which requires more frames of data for greater accuracy.

⁵It is worth mentioning that our method can still achieve satisfactory performance without these conditions, as demonstrated by the simulation results in Section V. These conditions are specifically raised for simplifying the analysis.

Additionally, we observe an interesting case: if N_f is even and $L = 1$, \mathbf{F}_2 is a scalar, which satisfies

$$\mathbf{F}_2 = \frac{1}{N_f} \left[\sum_{n=1}^{N_f} (-1)^n \right] \left[\sum_{n=1}^{N_f} (-1)^{n-1} \right] = 0 \quad (63)$$

This implies that for the $L = 1$ model, the CRLB can be reached if condition (a) is satisfied under these circumstances.

2) *MSE for Localization*: Next, we analyze the theoretical MSE for localization. The localization method takes as input a vector of TDOA estimates along with their covariance matrix. We have derived the variance of individual instantaneous TDOA estimates and demonstrated that they can approach the CRLB under certain conditions. The next step is to determine the covariance between different TDOA estimates.

We consider the errors of two TDOA estimates $\tau_{u;i1}$ and $\tau_{u;j1}$ ($i, j \in \mathcal{N}_a$, $i \neq j$ and $i, j \neq 1$)

$$\begin{aligned} \Delta \tau_{u;i1} &= \mathbf{V}_u \Delta \gamma_{u;i1} \\ &= \mathbf{V}_u \left(\mathbf{A}_{u;i1}^T \Sigma_{\eta_{u;i1}}^{-1} \mathbf{A}_{u;i1} \right)^{-1} \mathbf{A}_{u;i1}^T \Sigma_{\eta_{u;i1}}^{-1} \Delta \eta_{u;i1} \\ \Delta \tau_{u;j1} &= \mathbf{V}_u \Delta \gamma_{u;j1} \\ &= \mathbf{V}_u \left(\mathbf{A}_{u;j1}^T \Sigma_{\eta_{u;j1}}^{-1} \mathbf{A}_{u;j1} \right)^{-1} \mathbf{A}_{u;j1}^T \Sigma_{\eta_{u;j1}}^{-1} \Delta \eta_{u;j1} \end{aligned} \quad (64)$$

Thereby, their covariance matrix can be calculated by

$$\begin{aligned} \Sigma_{\tau_{u;i1}, \tau_{u;j1}} &= \mathbb{E} \{ \Delta \tau_{u;i1} \Delta \tau_{u;j1}^T \} \\ &= \mathbf{V}_u \left(\mathbf{A}_{u;i1}^T \Sigma_{\eta_{u;i1}}^{-1} \mathbf{A}_{u;i1} \right)^{-1} \mathbf{A}_{u;i1}^T \Sigma_{\eta_{u;i1}}^{-1} \mathbb{E} \{ \Delta \eta_{u;i1} \Delta \eta_{u;j1}^T \} \\ &\quad \Sigma_{\eta_{u;j1}}^{-1} \mathbf{A}_{u;j1} \left(\mathbf{A}_{u;j1}^T \Sigma_{\eta_{u;j1}}^{-1} \mathbf{A}_{u;j1} \right)^{-1} \mathbf{V}_u^T \end{aligned} \quad (65)$$

where

$$\begin{aligned} \Sigma_{\eta_{u;i1}, \tau_{u;j1}} &= \mathbb{E} \{ \Delta \eta_{u;i1} \Delta \eta_{u;j1}^T \} \\ &= \mathbf{C}_{u;i1}^{\phi_1} \Sigma_{\phi_1} \mathbf{C}_{u;j1}^{\phi_1 T} + \mathbf{C}_{u;i1}^{v_1} \Sigma_{v_1} \mathbf{C}_{u;j1}^{v_1 T} + \mathbf{C}_{u;i1}^{w_{u1}} \Sigma_{w_{u1}} \mathbf{C}_{u;j1}^{w_{u1} T} \end{aligned} \quad (66)$$

If conditions (a) and (b) for the instantaneous TDOA estimates to reach CRLB hold, similar to $\Sigma_{\tau_{u;ij}}$, we derive that:

$$\begin{aligned} \Sigma_{\tau_{u;i1}, \tau_{u;j1}} &\approx \frac{1}{2} \sigma_n^2 \mathbf{V}_u \left(\mathbf{V}_u^T \mathbf{V}_u \right)^{-1} \mathbf{V}_u^T \\ &\approx \frac{1}{2} \Sigma_{\tau_{u;i1}} \approx \frac{1}{2} \Sigma_{\tau_{u;ij}} \end{aligned} \quad (67)$$

Therefore, the actual covariance matrix of instantaneous TDOA estimates can approach the ideal covariance matrix obtained in the case of concurrent TOA measurements, as shown in (48). The methods in [27] is a two-step WLS method consisting of a series of linear operations. The estimated position error can be expressed as

$$\Delta \mathbf{p}_u^{(m)} = \mathbf{G}_1 \Delta \tau_u^{(m)} + \mathbf{G}_2 \Delta \mathbf{p}_a \quad (68)$$

where $\Delta \tau_u^{(m)} = [\Delta \tau_{u;21}^{(m)}, \Delta \tau_{u;31}^{(m)}, \dots, \Delta \tau_{u;N_a 1}^{(m)}]^T$ is the errors of TDOA estimates in Frame m , and $\Delta \mathbf{p}_a = [\Delta \mathbf{p}_1^T, \Delta \mathbf{p}_2^T, \dots, \Delta \mathbf{p}_{N_a}^T]^T$ is the errors in the anchors' position estimates. Detailed expressions of \mathbf{G}_1 and \mathbf{G}_2 can be found in [27]. As the TDOA estimates provided by P-TDOA are unbiased and the errors of anchors' position estimates are

zero-mean, the final position estimates are also unbiased. The covariance of position estimate $\mathbf{p}_u^{(m)}$ can be calculated as

$$\Sigma_{\mathbf{p}_u^{(m)}} = \mathbf{G}_1 \mathbf{Q}_u^{(m)} \mathbf{G}_1^T + \mathbf{G}_2 \Sigma_{\mathbf{p}_a} \mathbf{G}_2^T \quad (69)$$

where $\Sigma_{\mathbf{p}_a} = \text{diag}(\Sigma_{\mathbf{p}_1}, \Sigma_{\mathbf{p}_2}, \dots, \Sigma_{\mathbf{p}_{N_a}})$

In addition, as demonstrated by Sun, the localization method can achieve the CRLB under small noise conditions [27]. We have shown that the covariance matrix of instantaneous TDOA estimates can approach the ideal scenario of concurrent TOA measurements. Therefore, if conditions (a) and (b) hold, our proposed localization method can also approach the CRLB of concurrent TOA measurements in the presence of small noise.

V. NUMERICAL SIMULATION

In this section, we conduct comprehensive numerical simulations to validate the effectiveness of our proposed methods for TDOA estimation and mobile target localization. We consider a 2D simulation scenario ($K=2$) involving a positioning system composed of N_a stationary anchors and one mobile target u . The noise of clock drifts (ω) and initial clock offsets (ϕ) of the nodes are random variables drawn from uniform distributions, specifically, $\omega \sim \mathcal{U}[-20, 20]$ parts per million (ppm) [21] and $\phi \sim \mathcal{U}[-1, 1]$ ms. The frame length T_f is set to 0.1s and each frame is divided into $N_s=20$ time slots whose duration is $T_s=5$ ms. Other parameters are specified in respective experiments.

A. TDOA Estimation

We select two classical and effective TDOA estimation methods as benchmarks for comparison:

- **Benchmark 1** (Asynchronous Time Difference of Arrival (A-TDOA) [16] [19]) : A classical TDOA estimation method which requires CFO measurement assistance. Specifically, [19] discusses the uplink TDOA cases where tags transmit blink messages, while [16] extends the method to downlink TDOA cases, which is the focus of our problem.
- **Benchmark 2** (Signal-Multiplexing Network Ranging (SM-NR) [21]): A new and effective network ranging method which is capable of both active ranging and differential ranging.

As several other TDOA estimation methods [20], [36], [37] have been shown to be inferior to SM-NR [21], the selection of these benchmarks is appropriate and justified. Additionally, since P-TDOA utilizes information from multiple frames for estimation, whereas the benchmarks use only a single frame, we apply polynomial fitting to the raw TDOA estimates of the benchmarks for a fair comparison. This allows TDOAs to be estimated using a uniform polynomial model as in (8). We refer to the fitting versions of the benchmarks as ‘A-TDOA fitting’ and ‘SM-NR fitting’, respectively.

Unless otherwise specified, we assume that Target u is located at $(0, 0)$ initially and $N_a=10$ anchors are all randomly placed within a square centering at $(0, 0)$ with sides length 2 km. The anchors remain stationary, while Target u moves with a constant velocity in a random direction. The

speed is drawn from a uniform distribution independently, i.e., $v \sim \mathcal{U}[-v_{\max}, +v_{\max}]$, with $v_{\max}=10$ m/s. The transmission times are set by the anchors themselves, and the noise in the transmission stamps is generally only caused by clock jitter and can be neglected, which is a typical case in UWB systems [31], [38]. Therefore, we set $\sigma_t = 0$, and the variance of the noise of reception timestamps is set as $\sigma_r^2 = -30$ dB [38]. The default standard deviation of clock offset errors is set to $\sigma_\phi = 10^{-11}$ s.

For different methods, unless otherwise specified, the model order L in P-TDOA is set to 2. Without loss of generality, we select Anchor 1 as the global clock reference node, serving as the ‘sync node’ in [21] as well. We assume that the CFO in A-TDOA is measured precisely with no measurement error. The fitting order for ‘A-TDOA fitting’ and ‘SM-NR fitting’ is set equal to L .

The RMSE of TDOA is given by

$$\text{RMSE}_{\text{TDOA}} = \mathbb{E} \left\{ \sqrt{\frac{1}{N_f} \sum_{(i,j) \in \mathcal{N}_p} \|\Delta \tau_{u;i,j}\|^2} \right\} \quad (70)$$

where $\Delta \tau_{u;i,j} = \hat{\tau}_{u;i,j} - \tau_{u;i,j}$ represents the TDOA estimation error across N_f frames. $\tau_{u;i,j}$ is the ground truth of the TDOA at the instants when Target u receives the signal from Anchor j . For P-TDOA, \mathbf{t}_u is selected as these moments for instantaneous TDOA estimation.

In the remainder of this subsection, we compare the performance of the proposed P-TDOA with the selected benchmarks both, as well as the CRLB for instantaneous TDOA estimation without and with the polynomial model (CRLB1 and CRLB2), in both static and dynamic scenarios for different anchor pairs. Additionally, we test the adaptability of P-TDOA to different types of motion and varying noise levels. For each type of experiments, we conduct $N_{\text{sim}} = 10000$ simulations, where the positions of anchors, target velocity and their clock parameters vary across different simulations.

1) *Adaptability to static scenarios:* Although the P-TDOA method is designed for dynamic scenarios, it also performs well in static scenarios. We set $L = 1$ for P-TDOA method and assume that the target remains stationary. The results are shown in Fig. 4. It is observed that the polynomial model can reduce the CRLB of TDOA estimation, and CRLB2 decreases with an increasing number of frames. Moreover, P-TDOA outperforms SM-NR, A-TDOA, and their respective fitting versions, exceeding CRLB1 and asymptotically approaching CRLB2 in static scenarios.

Furthermore, we observe that when N_f is odd such as $N_f = 3, 5$ the theoretical RMSE of P-TDOA shows a slight gap compared to CRLB2 whereas when N_f is even, they are extremely close, which confirms the observation in (63). And the gap diminishes with the increase of N_f when $N_f = 7, 9$, validating the previously mentioned condition (b) for the theoretical MSE to reach CRLB.

2) *Adaptability to different anchor pairs:* From this part, we focus on evaluating the performance of P-TDOA in dynamic scenarios. As mentioned above, larger transmission intervals may cause the QSA to fail. Consequently, different transmission intervals between different anchor pairs lead to different

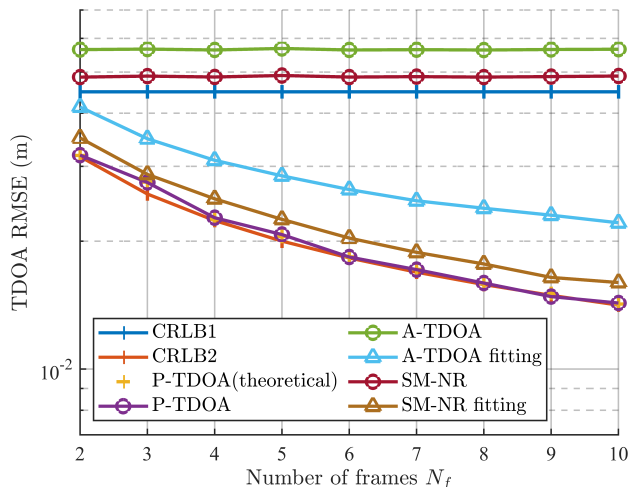


Fig. 4: TDOA estimation performance comparison in static scenarios. The polynomial model can reduce the CRLB of TDOA estimation, and CRLB2 decreases with an increasing number of frames. Moreover, P-TDOA outperforms all benchmarks, exceeding CRLB1 and asymptotically approaching CRLB2

TDOA estimation performances. We consider three sets of anchor pairs:

- ① Set 1: $\mathcal{N}_p = \{(1, 2)\}$
- ② Set 2: $\mathcal{N}_p = \{(1, j), j \in \mathcal{N}_a \ \& \ j \neq 1\}$
- ③ Set 3: $\mathcal{N}_p = \{(i, j), i, j \in \mathcal{N}_a \ \& \ i < j\}$

The performance of the TDOA estimation of different methods for each set is shown in Fig. 5. The results demonstrate that the proposed P-TDOA method outperforms A-TDOA and SM-NR in all three sets, even when fitting techniques are applied. Moreover, P-TDOA can asymptotically reach CRLB2. The slight deviation from the theoretical RMSE is attributed to increased nonlinearity as the number of frames increases. While an increased number of frames can improve estimation precision, it also increases the risk of model mismatch.

For the comparison of other methods, we provide the following analysis. A-TDOA performs relatively well in Set 1, and its performance improves with the fitting techniques as the number of frames increases, as shown in Fig. 5(a). This is because, in Set 1, the transmission intervals between Anchor 1 and Anchor 2 are relatively short, allowing the displacement of Target u or the variation of the TDOAs to be neglected. However, for other anchor pairs with longer transmission intervals in Set 2 and Set 3, A-TDOA produces biased TDOA estimates, leading to increased RMSEs, as shown in Fig. 5(b) and Fig. 5(c). A similar trend is observed for SM-NR. Although SM-NR performs well for anchor pairs that include the ‘sync node,’ its performance degrades for other anchor pairs.

We compare the TDOA estimation results for all anchor pairs ($N_p = \binom{N_a}{2} = 45$) in Set 3 with $N_f = 5$, as shown in Fig. 6. The x-axis represents the indices of the anchor pairs, referred to as the pair index, ranging from 1 to N_p , following lexicographic order. Specifically, anchor pair (1, 2) is indexed as 1, where the first element remains unchanged while the

second element increments by one each time. The first element increments only after the second element reaches its maximum value. For example, the anchor pairs in Set 3 follow the order (1, 2), (1, 3), ..., (1, 10), (2, 3), ..., (8, 10), (9, 10).

Fig. 6 shows that the proposed P-TDOA method outperforms the benchmark methods by providing lower and more stable TDOA estimation RMSEs. Notably, we select two representative anchor pairs, (2, 3) and (2, 10), and use red ellipses to highlight the error points of A-TDOA, SM-NR, and their fitting versions. We observe that the TDOA estimation performance of A-TDOA deteriorates as the transmission intervals between anchors increase, indicating the invalidity of QSA over larger intervals. SM-NR exhibits a similar pattern as A-TDOA for anchor pairs without the sync node. In contrast, while the precision of TDOA estimates across different anchor pairs varies slightly for P-TDOA, this variation is far less significant than that seen in A-TDOA and SM-NR. This enables Target u to obtain precise TDOA estimates for all anchor pairs. The proposed P-TDOA method proves effective for network differential ranging in dynamic scenarios.

3) *Adaptability to different motions*: Previous experiments have demonstrated that P-TDOA outperforms the benchmarks for TDOA estimation in dynamic scenarios. In this part, we evaluate the adaptability of P-TDOA to different types of motion. We consider three types of motion:

- ① Motion 1 (uniform linear motion) : The direction of movement is random, and the constant speed is independently drawn from a uniform distribution, i.e., $v \sim \mathcal{U}[v_{\max}, +v_{\max}]$ and $v_{\max} = 10\text{m/s}$, which is consistent with the motion used in previous experiments.
- ② Motion 2 (uniform circular motion) : The direction of movement is random, and the initial speed is independently drawn from a uniform distribution, i.e., $v \sim \mathcal{U}[v_{\max}, +v_{\max}]$ and $v_{\max} = 10\text{m/s}$. The circle radius $R \sim \mathcal{U}[0, R_{\max}]$, with $R_{\max} = 100\text{m}$.
- ③ Motion 3 (uniformly accelerated linear motion) : The direction of movement is random, and the initial speed is independently drawn from a uniform distribution, i.e., $v \sim \mathcal{U}[v_{\max}, +v_{\max}]$ and $v_{\max} = 10\text{m/s}$. The acceleration $a \sim \mathcal{U}[0, a_{\max}]$, with $a_{\max} = 5 \text{ m/s}^2$.

For each type of motion, we apply $L = 2$ and $L = 3$ for comparison. The results are shown in Fig. 7.

We observe that the theoretical RMSEs for lower-order $L = 2$ are smaller than those for higher-order $L = 3$ across all three types of motion. If the model accurately captures the nonlinear variation of TDOAs, the estimation precision improves with an increasing number of frames, as seen in both the $L = 2$ and $L = 3$ cases for Motion 1, and in the $L = 3$ case for Motion 3. However, if the model fails to match the nonlinear variation of TDOAs, the actual RMSEs deviate from the theoretical values, and an increased number of frames may degrade estimation performance, as demonstrated by both the $L = 2$ and $L = 3$ cases in Motion 2 and the $L = 2$ case in Motion 3. Therefore, in practical implementation, careful selection of the model order and the number of frames for estimation is crucial. A feasible approach is Order Recursive Least Squares (ORLS) as discussed in [28], [35], which is

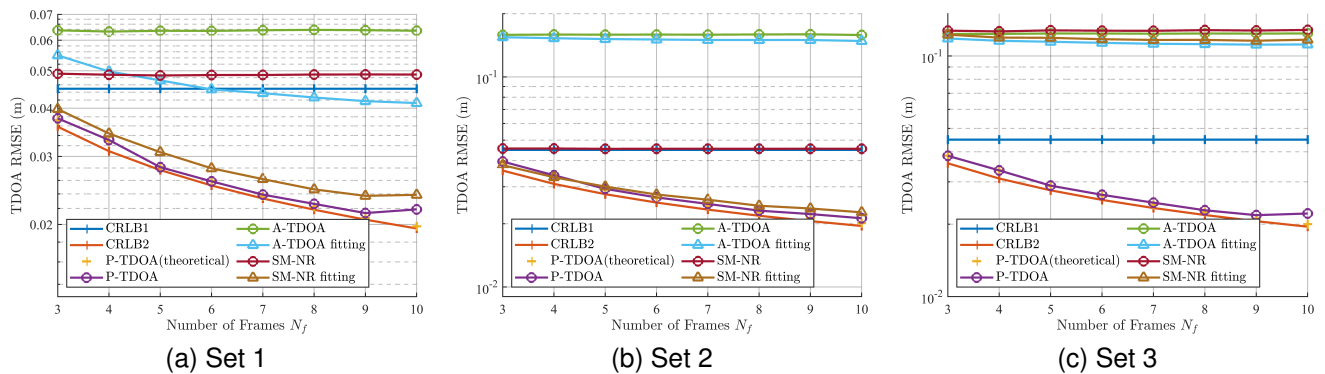


Fig. 5: TDOA estimation performance comparison versus different set of anchor pairs (a) Set 1: $\mathcal{N}_p = \{(1, 2)\}$. (b) Set 2: $\mathcal{N}_p = \{(1, j)\}, j \in \mathcal{N}_a \& j \neq 1$. (c) Set 3: $\mathcal{N}_p = \{(i, j)\}, i, j \in \mathcal{N}_a \& i < j$. P-TDOA outperforms all benchmarks in three sets of anchor pairs and can asymptotically reach CRLB2. The slight deviation from the theoretical RMSE is attributed to increased nonlinearity as the number of frames increases.

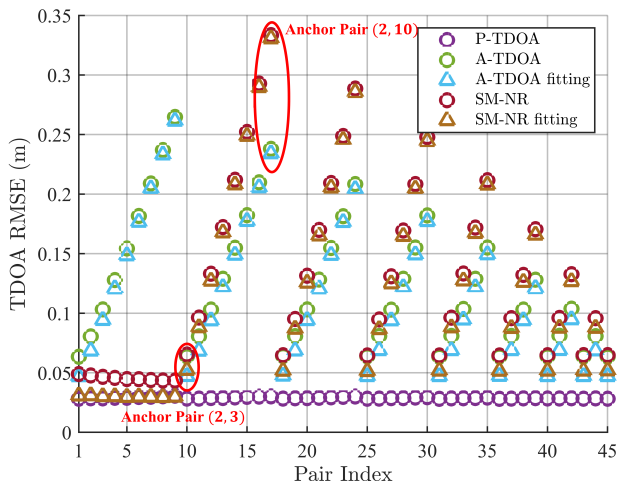


Fig. 6: TDOA estimation performance comparison for different anchor pairs in Set 3 with $N_f = 5$. P-TDOA outperforms all benchmarks by providing lower and more stable TDOA estimation RMSEs all anchor pairs.

beyond the scope of this paper and will not be elaborated further.

4) *Adaptability to different noise:* In this section, we analyze the impact of different levels of timestamp noise and synchronization errors on TDOA estimation. For all experiments, we set $L = 2$ and $N_f = 3$. Fig. 8 presents the TDOA estimation performance of P-TDOA under varying levels of timestamp noise and synchronization errors. The results validate the accuracy of our theoretical analysis and demonstrate the effectiveness of the proposed P-TDOA method, which remains robust across different noise levels, surpassing CRLB1 and approaching CRLB2.

B. Mobile Target Localization

We select two recent sequential TOA-based mobile target localization methods as benchmarks for comparison. Their settings and range of utilization are similar to those of our

proposed method. Mobile targets only need to passively receive signals transmitted by anchors, allowing the system to serve an unlimited number of targets.

- **Benchmark 1** (Closed-Form Joint Localization and Synchronization (CFJLAS) [24]): An effective mobile target localization method based on sequential TOAs of one-way broadcast signals, which assumes that the mobile target moves at a constant velocity during one frame and jointly estimates the position, velocity and clock parameters together.
- **Benchmark 2** (Timestamp-Conversion-based Joint Localization and Synchronization (TCJLAS) [25]): a novel timestamp-conversion method that employs Lagrange interpolation to convert sequential measurements to concurrent measurements for joint localization and synchronization.

We also derive the CRLB of localization for comparison. If the covariance matrix follows (46), the derived CRLB is denoted as CRLB1, and if the covariance matrix follows (48), which utilizes TDOA estimates with the polynomial model, the derived CRLB is denoted as CRLB2.

The default system setting is the same as those in Section V-A, with the model order of P-TDOA set to $L = 2$ and the number of frames set to $N_f = 3$. The standard deviation of each anchor's position error is set to $\sigma_p = 0.1\text{m}$ and $\Sigma_{\mathbf{p}_i} = \text{diag}([\sigma_p^2, \sigma_p^2])$. Since the anchors are randomly placed, the solution may degrade for certain anchor distributions. To better evaluate the performance of different methods, we exclude outliers based on unified thresholds.

The RMSE of position is given by

$$\text{RMSE}_{\mathbf{p}} = \mathbb{E} \{ \|\hat{\mathbf{p}} - \mathbf{p}_{\text{true}}\| \} \quad (71)$$

where $\hat{\mathbf{p}}$ denotes the estimated position and \mathbf{p}_{true} denotes the true position of the target. The ground truth of position is taken as the instantaneous position at the start of each frame, and t_u is selected as those moments for P-TDOA estimation in (8). For each type of experiment, we conduct $N_{\text{sim}} = 10000$ simulations, where the positions, velocity and clock parameters vary as well.

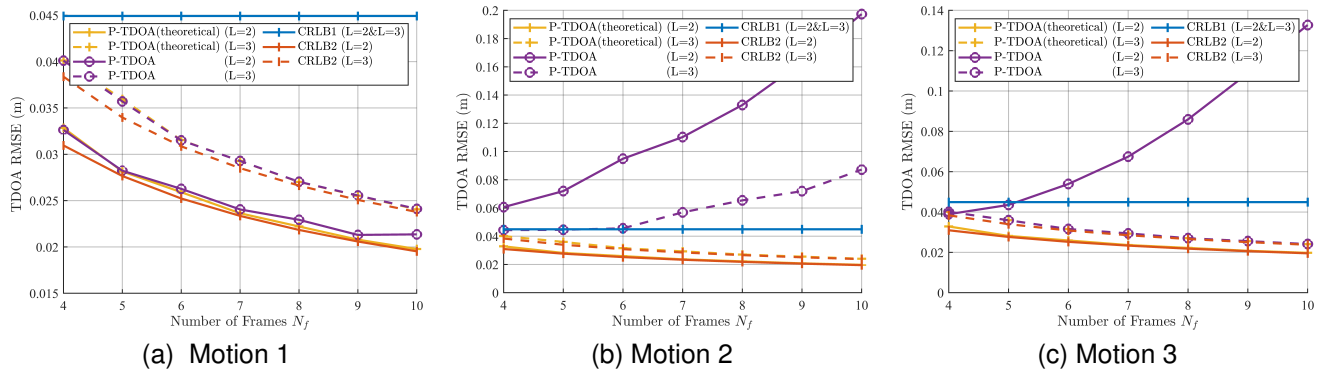


Fig. 7: TDOA estimation performance comparison versus different types of motion (a) Motion 1: uniform linear motion. (b) Motion 2: uniform circular motion. (c) Motion 3: uniformly accelerated linear motion. The theoretical RMSEs for lower-order $L = 2$ are smaller than those for higher-order $L = 3$ across all three types of motion while low-order model may encounter mismatch in high-dynamic scenarios.

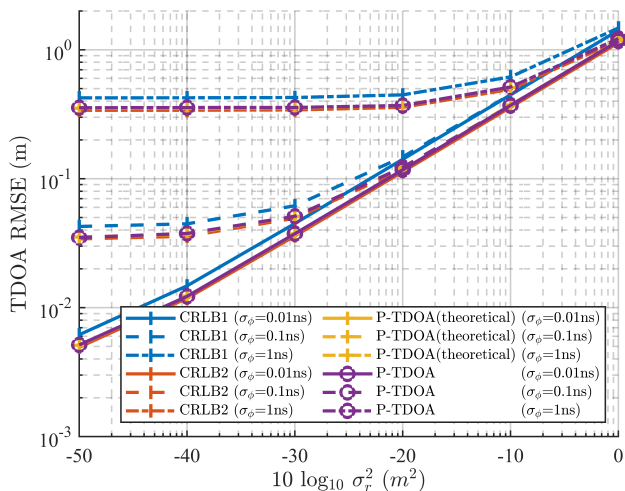


Fig. 8: TDOA estimation performance of P-TDOA versus different levels of noise. The results validate the accuracy of our theoretical analysis and demonstrate the effectiveness of the proposed P-TDOA method across different noise levels.

1) *Performance versus different levels of noise:* We set the reception timestamp noise to range from 0 m to 1 m, increasing in increments of 0.1 m. Fig. 9 illustrates the RMSE of position estimates under varying noise levels. It is evident that the polynomial model used for TDOA estimates also affects the CRLB for localization. The proposed P-TDOA method outperforms the benchmark methods, surpassing CRLB1 and approaching CRLB2 under small noise conditions, which aligns with the characteristics of the TDOA-based localization method described in [27].

2) *Performance versus different number of anchors:* The number of anchors significantly impacts localization performance. We vary the number of anchors from 4 to 12, and the resulting position estimation RMSEs are presented in Fig. 9. The proposed P-TDOA method and TCJLAS require a minimum of four anchors to achieve stable solutions, while CFJLAS requires at least seven anchors due to the joint

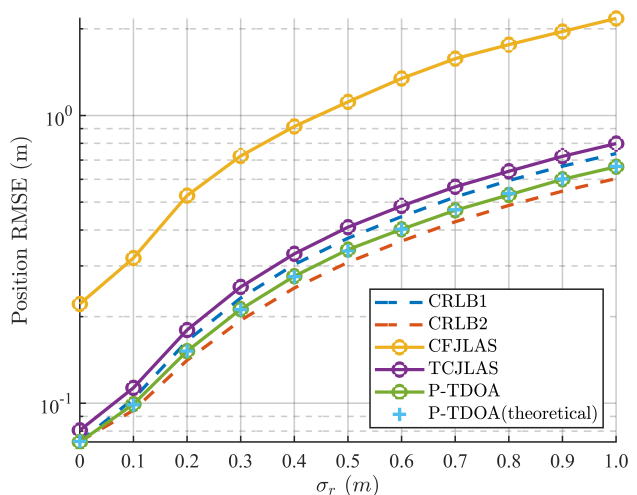


Fig. 9: Localization performance versus different levels of noise. The polynomial model used for TDOA estimates also affects the CRLB for localization. The proposed P-TDOA method outperforms all benchmarks, surpassing CRLB1 and approaching CRLB2 under small noise conditions.

estimation of additional parameters. With the same number of anchors, P-TDOA consistently outperforms the benchmarks, and the localization accuracy improves as the number of anchors increases. Therefore, P-TDOA not only reduces the anchor requirement but also achieves superior performance with a fixed number of anchors.

The reduced anchor requirement is attributed to the decoupling of localization from synchronization and target dynamics. Our proposed method leverages multiple frames of data to eliminate the unknown clock parameters of Target u in (12) to (14) and to capture the dynamics of TDOAs. Essentially, our approach trades longer observation time for fewer anchor requirements. Since maintaining a stable topology over short periods is more feasible than establishing multiple connections, our method is well-suited for a broader range of application scenarios.

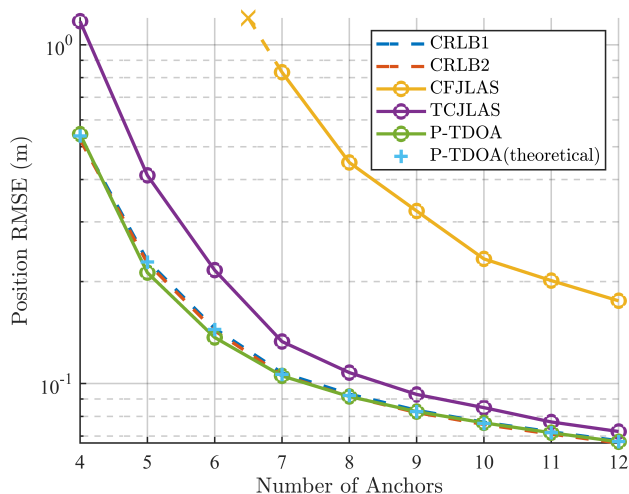


Fig. 10: Localization performance versus different number of anchors. The X marks indicate that the methods don't work with a smaller number of anchors. P-TDOA and TCJLAS requires at least 4 anchors while CFJLAS requires at least 7 anchors. With the same number of anchors, the localization accuracy of P-TDOA is higher than all benchmarks.

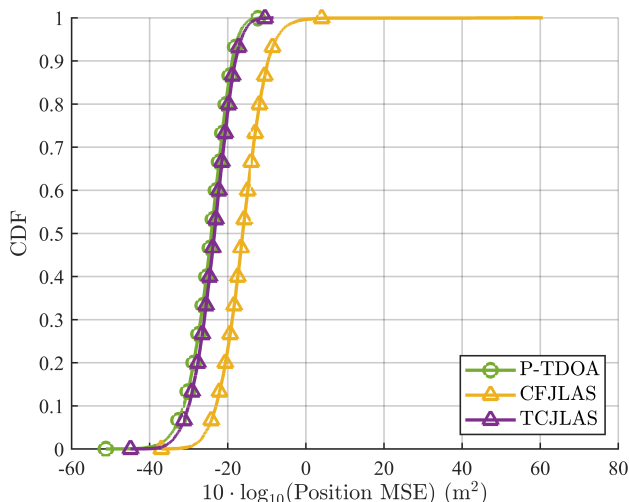


Fig. 11: Localization performance versus different anchor distributions. P-TDOA exhibits higher robustness to different anchor distributions compared to benchmarks.

3) *Performance versus different anchor distributions:* The spatial distributions of the anchors significantly influence localization performance. To assess the adaptability of the methods to varying positional distributions, we conduct extensive evaluations. Fig. 11 presents the cumulative distribution function (CDF) of the estimated position MSE. It is evident that the curve for the proposed P-TDOA method is the steepest among all compared methods and achieves the lowest estimation MSE when the CDF reaches 1. This result highlights the superior adaptability and robustness of P-TDOA to different anchor distributions.

4) *Performance under high dynamics of the target:* In the aforementioned localization experiments, the target is assumed to move with constant velocity. However, there are many

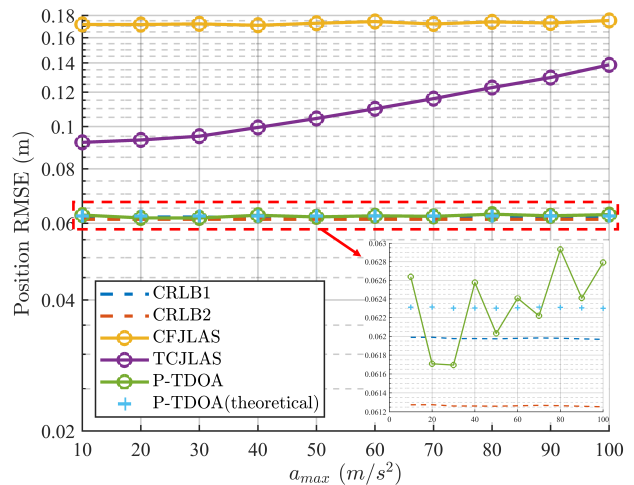


Fig. 12: Localization performance versus high dynamics of the target. P-TDOA with higher-order model can be adapted to localization for targets with high dynamics while the performances of benchmarks with the constant velocity assumption degrade.

scenarios in which mobile targets exhibit high dynamics, such as during takeoff or landing. Here, we assume the target undergoes uniformly accelerated linear motion with high dynamics, where the direction of movement is random, and the initial speed is independently drawn from a uniform distribution, i.e., $v \sim \mathcal{U}[v_{\max}, +v_{\max}]$ and $v_{\max} = 100\text{m/s}$. The acceleration $a \sim \mathcal{U}[0, a_{\max}]$. We set the a_{\max} ranging from 10 m/s^2 to 100 m/s^2 , increasing in increments of 10 m/s^2 steps.

We set $L = 3$ and $N_f = 4$ for P-TDOA. Fig. 12 shows the position estimation RMSEs for varying accelerations. The results indicate that P-TDOA outperforms the benchmark methods in high-dynamic scenarios. Moreover, we observe that the performance of TCJLAS degrades with increasing acceleration. This degradation occurs because TCJLAS assumes a constant speed within each frame, which is unsuitable for high-dynamic scenarios. Although CFJLAS also assumes constant speed, the duration for constant speed is limited to $N_a T_s < N T_s = T_f$, which mitigates the impact of acceleration compared to TCJLAS.

VI. CONCLUSION

In this paper, we propose a novel and effective TDOA estimation method named P-TDOA and develop a localization method for mobile targets in dynamic scenarios.

P-TDOA employs a polynomial model to approximate time-varying TDOAs. We introduce a weighted least squares (WLS) method called MWLS and an equation construction strategy named STDS to estimate model parameters and subsequently obtain instantaneous TDOAs. Our proposed method is capable of estimating instantaneous TDOAs at any arbitrary time within the measurement period, allowing for the estimation of instantaneous TDOAs for different anchor pairs simultaneously. Extensive simulations validate that the proposed P-TDOA method outperforms existing methods in both static and dynamic scenarios and approaches the CRLB for instantaneous TDOA estimation.

Building upon the simultaneously estimated instantaneous TDOAs obtained by P-TDOA, we establish an efficient down-link mobile target localization method. The newly proposed method decouples the unknown position parameters from other parameters, offering several advantages over state-of-the-art sequential TOA-based methods. Firstly, it achieves higher localization accuracy. Secondly, it reduces the number of required anchors, with only four anchors being sufficient in 2D scenarios. Lastly, the complete solution process requires only simple linear operations, avoiding complex nonlinear optimization or iterations, making the method computationally efficient and easy to implement.

Regarding future work, several issues warrant further research. First, the proposed P-TDOA method utilizes several frames of data, which impacts real-time capability. We will further investigate how to enhance the adaptability and efficiency of P-TDOA in real-time applications. Additionally, while P-TDOA eliminates the unknown clock parameters of mobile targets and focuses on localization, clock synchronization for passive targets remains unresolved. It is worth exploring how to achieve clock synchronization within the framework of P-TDOA.

ACKNOWLEDGMENTS

This work is supported by the National Key R&D Program of China under Grant No. 2021YFA0716603 and the National Natural Science Foundation of China under Grant No. U2233217.

REFERENCES

- [1] M. Martalò, S. Perri, G. Verdano, F. De Mola, F. Monica, and G. Ferrari, "Improved uwb tdoa-based positioning using a single hotspot for industrial iot applications," *IEEE Transactions on Industrial Informatics*, vol. 18, no. 6, pp. 3915–3925, 2021.
- [2] J. Wyffels, J. De Brabanter, P. Crombez, P. Verhoeve, B. Nauwelaers, and L. De Strycker, "Distributed, signal strength-based indoor localization algorithm for use in healthcare environments," *IEEE journal of biomedical and health informatics*, vol. 18, no. 6, pp. 1887–1893, 2014.
- [3] Y. Zhang, Y. Ma, K. Liu, J. Wang, and S. Li, "Rfid based vehicular localization for intelligent transportation systems," in *2019 IEEE International Conference on RFID Technology and Applications (RFID-TA)*. IEEE, 2019, pp. 267–272.
- [4] T. Alhmiedat, A. A. Taleb, and M. Bsoul, "A study on threats detection and tracking systems for military applications using wsns," *International Journal of Computer Applications*, vol. 40, no. 15, pp. 12–18, 2012.
- [5] E. D. Kaplan and C. Hegarty, *Understanding GPS/GNSS: principles and applications*. Artech house, 2017.
- [6] B. Hofmann-Wellenhof, H. Lichtenegger, and E. Wasle, *GNSS—global navigation satellite systems: GPS, GLONASS, Galileo, and more*. Springer Science & Business Media, 2007.
- [7] A. Chehri, P. Fortier, and P. M. Tardif, "Uwb-based sensor networks for localization in mining environments," *Ad Hoc Networks*, vol. 7, no. 5, pp. 987–1000, 2009.
- [8] S. Krishnan, P. Sharma, Z. Guoping, and O. H. Woon, "A uwb based localization system for indoor robot navigation," in *2007 IEEE International Conference on Ultra-Wideband*. IEEE, 2007, pp. 77–82.
- [9] L. Zwirello, T. Schipper, M. Harter, and T. Zwick, "Uwb localization system for indoor applications: Concept, realization and analysis," *Journal of Electrical and Computer Engineering*, vol. 2012, no. 1, p. 849638, 2012.
- [10] E. Xu, Z. Ding, and S. Dasgupta, "Source localization in wireless sensor networks from signal time-of-arrival measurements," *IEEE Transactions on Signal Processing*, vol. 59, no. 6, pp. 2887–2897, 2011.
- [11] H. Shen, Z. Ding, S. Dasgupta, and C. Zhao, "Multiple source localization in wireless sensor networks based on time of arrival measurement," *IEEE Transactions on Signal Processing*, vol. 62, no. 8, pp. 1938–1949, 2014.
- [12] R. M. Vaghefi and R. M. Buehrer, "Asynchronous time-of-arrival-based source localization," in *2013 IEEE International Conference on Acoustics, Speech and Signal Processing*. IEEE, 2013, pp. 4086–4090.
- [13] T. Wang, H. Ding, H. Xiong, and L. Zheng, "A compensated multi-anchors tof-based localization algorithm for asynchronous wireless sensor networks," *IEEE Access*, vol. 7, pp. 64 162–64 176, 2019.
- [14] A. Ledergerber, M. Hamer, and R. D'Andrea, "A robot self-localization system using one-way ultra-wideband communication," in *2015 IEEE/RSJ International Conference on Intelligent Robots and Systems (IROS)*. IEEE, 2015, pp. 3131–3137.
- [15] J. Tiemann and C. Wietfeld, "Scalable and precise multi-uav indoor navigation using tdoa-based uwb localization," in *2017 international conference on indoor positioning and indoor navigation (IPIN)*. IEEE, 2017, pp. 1–7.
- [16] G.-C. Pătru, L. Flueraț, I. Vasilescu, D. Niculescu, and D. Rosner, "Flextdoa: Robust and scalable time-difference of arrival localization using ultra-wideband devices," *IEEE Access*, vol. 11, pp. 28 610–28 627, 2023.
- [17] D. Neirynek, E. Luk, and M. McLaughlin, "An alternative double-sided two-way ranging method," in *2016 13th workshop on positioning, navigation and communications (WPNC)*. IEEE, 2016, pp. 1–4.
- [18] A. Toky, R. P. Singh, and S. Das, "Localization schemes for underwater acoustic sensor networks—a review," *Computer Science Review*, vol. 37, p. 100241, 2020.
- [19] I. Dotlic, A. Connell, and M. McLaughlin, "Ranging methods utilizing carrier frequency offset estimation," in *2018 15th Workshop on Positioning, Navigation and Communications (WPNC)*. IEEE, 2018, pp. 1–6.
- [20] Z. Zhang, H. Zhao, and Y. Shen, "High-efficient ranging algorithms for wireless sensor network," in *2019 11th International Conference on Wireless Communications and Signal Processing (WCSP)*. IEEE, 2019, pp. 1–6.
- [21] Z. Zhang, H. Zhao, J. Wang, and Y. Shen, "Signal-multiplexing ranging for network localization," *IEEE Transactions on Wireless Communications*, vol. 21, no. 3, pp. 1694–1709, 2021.
- [22] Q. Shi, X. Cui, S. Zhao, and M. Lu, "Sequential toa-based moving target localization in multi-agent networks," *IEEE Communications Letters*, vol. 24, no. 8, pp. 1719–1723, 2020.
- [23] S. Zhao, X.-P. Zhang, X. Cui, and M. Lu, "Optimal localization with sequential pseudorange measurements for moving users in a time-division broadcast positioning system," *IEEE Internet of Things Journal*, vol. 8, no. 11, pp. 8883–8896, 2021.
- [24] N. Guo, S. Zhao, X.-P. Zhang, Z. Yao, X. Cui, and M. Lu, "New closed-form joint localization and synchronization using sequential one-way toas," *IEEE Transactions on Signal Processing*, vol. 70, pp. 2078–2092, 2022.
- [25] J. Sun, Y. Wang, and Y. Shen, "A novel timestamp-conversion-based localization and synchronization method for moving users using sequential measurements," *IEEE Transactions on Vehicular Technology*, 2024.
- [26] Y. T. Chan and K. C. Ho, "A simple and efficient estimator for hyperbolic location," *IEEE transactions on signal processing*, vol. 42, no. 8, pp. 1905–1915, 1994.
- [27] M. Sun and K. Ho, "An asymptotically efficient estimator for tdoa and fdoa positioning of multiple disjoint sources in the presence of sensor location uncertainties," *IEEE Transactions on Signal Processing*, vol. 59, no. 7, pp. 3434–3440, 2011.
- [28] R. T. Rajan and A.-J. van der Veen, "Joint ranging and synchronization for an anchorless network of mobile nodes," *IEEE Transactions on Signal Processing*, vol. 63, no. 8, pp. 1925–1940, 2015.
- [29] C. Sahu, M. Banavar, and J. Sun, "Data-driven nonlinear tdoa for accurate source localization in complex signal dynamics," *IEEE Sensors Journal*, 2024.
- [30] N. M. Freris, S. R. Graham, and P. Kumar, "Fundamental limits on synchronizing clocks over networks," *IEEE Transactions on Automatic Control*, vol. 56, no. 6, pp. 1352–1364, 2010.
- [31] Q. Shi, X. Cui, S. Zhao, S. Xu, and M. Lu, "Blas: Broadcast relative localization and clock synchronization for dynamic dense multiagent systems," *IEEE Transactions on Aerospace and Electronic Systems*, vol. 56, no. 5, pp. 3822–3839, 2020.
- [32] A. A. Ghany, B. Uguen, and D. Lemur, "A parametric tdoa technique in the iot localization context," in *2019 16th Workshop on Positioning, Navigation and Communications (WPNC)*. IEEE, 2019, pp. 1–6.
- [33] I. Kravets, O. Kapshii, O. Shuparskyy, and A. Luchechko, "A new parametric three stage weighted least squares algorithm for tdoa-based localization," *IEEE Access*, 2024.
- [34] X.-D. Zhang, *Matrix analysis and applications*. Cambridge University Press, 2017.

- [35] S. M. Kay, *Fundamentals of statistical signal processing: estimation theory*. Prentice-Hall, Inc., 1993.
- [36] K. A. Horváth, G. III, and Á. Milánkovich, "Passive extended double-sided two-way ranging algorithm for uwb positioning," in *2017 Ninth International Conference on Ubiquitous and Future Networks (ICUFN)*. IEEE, 2017, pp. 482–487.
- [37] K. A. Horvath, G. III, and Á. Milánkovich, "Passive extended double-sided two-way ranging with alternative calculation," in *2017 IEEE 17th International Conference on Ubiquitous Wireless Broadband (ICUWB)*. IEEE, 2017, pp. 1–5.
- [38] C. Xu and C. L. Law, "Delay-dependent threshold selection for uwb toa estimation," *IEEE communications letters*, vol. 12, no. 5, pp. 380–382, 2008.



Chenxin Tu received the B.E. degree in electronic engineering from Tsinghua University, Beijing, China, in 2022, where he is currently pursuing the Ph.D. degree with the Department of Electronic Engineering.

His current research interests include wireless localization and cooperative localization.



Xiaowei Cui received the B.S. and Ph.D. degrees in electronic engineering from Tsinghua University, Beijing, China, in 2000 and 2005, respectively. Since 2005, he has been with the Department of Electronic Engineering, Tsinghua University, where he is currently a Professor.

His research interests include robust GNSS signal processing, multipath mitigation techniques, and high-precision positioning. He is a member of the Expert Group of China BeiDou Navigation Satellite System.



Gang Liu is an associate researcher at the Department of Electronic Engineering, Tsinghua University, China. His research interests include GNSS/INS integrated navigation techniques, and high-precision localization. He obtained both the BS and PhD degrees in instrument science and technology from Tsinghua University in 2007 and 2015, respectively.



Sihao Zhao (Senior Member, IEEE) received the B.S. and Ph.D. degrees in electronic engineering from Tsinghua University, Beijing, China, in 2005 and 2011, respectively. He is currently a Senior Algorithm Designer with NovAtel, Autonomy and Positioning division of Hexagon, Calgary, AB, Canada. From 2011 to 2013, he was an Electronics Systems Engineer with China Academy of Space Technology, Beijing, China. From 2013 to 2019, he was a Post-doctoral Researcher and then an Assistant Professor with the Department of Electronic Engineering, Tsinghua University, Beijing, China. From 2020 to 2021, he was a Research Associate with the Department of Electrical, Computer and Biomedical Engineering, Toronto Metropolitan University, Toronto, ON, Canada.



Mingquan Lu is a Professor in the Department of Electronic Engineering at Tsinghua University. He directs the PNT Research Center, which develops GNSS and alternative PNT technologies. His current research focuses on GNSS signal processing, GNSS receiver development and emerging PNT technologies. He authored or co-authored 5 books and book chapters, published over 300 journal and conference papers, and hold nearly 100 patents. He provided numerous services to the GNSS community, including associate editor for *Satellite Navigation and Journal*

of Navigation and Positioning.

Dr. Lu is a fellow of ION and a recipient of the ION Thurlow Award. He provided numerous services to the GNSS community, including as an Associate Editor for *Satellite Navigation* and the *Journal of Navigation and Positioning*.